
SPARSE FEDERATED LEARNING WITH HIERARCHICAL PERSONALIZED MODELS

Xiaofeng Liu*, Yinchuan Li*, Yunfeng Shao, Qing Wang

ABSTRACT

Federated learning (FL) can achieve privacy-safe and reliable collaborative training without collecting users' private data. Its excellent privacy security potential promotes a wide range of FL applications in Internet-of-Things (IoT), wireless networks, mobile devices, and autonomous vehicles. However, the FL method suffers from poor model performance on non-IID data and excessive traffic volume. We propose a personalized FL algorithm using a hierarchical proximal mapping based on ℓ_2 -norm, named sparse federated learning with hierarchical personalized models (sFedHP), which significantly improves the global model performance facing diverse data. An approximated ℓ_1 -norm is well used as the sparse constraint to reduce the communication cost. Convergence analysis shows that sFedHP's convergence rate is state-of-the-art with linear speedup and the sparse constraint only reduces the convergence rate to a small extent while significantly reducing the communication cost. Experimentally, we demonstrate the benefits of sFedHP compared with the FedAvg, HierFAVG (hierarchical FedAvg), and personalized FL methods based on local customization, including FedAMP, FedProx, Per-FedAvg, pFedMe, and pFedGP.

1 Introduction

Machine learning methods have proliferated in real-life applications thanks to the tremendous number of labeled samples [1]. Typically, these samples collected on users' devices, such as mobile phones, are expected to send to a centralized server with mighty computing power to train a deep model [2]. However, users are often reluctant to share personal data due to privacy concerns, which motivates the emergence of federated learning (FL) [3]. Federated Averaging (FedAvg) [3] is known as the first FL algorithm to build a global model for different clients while protecting their data locally. Moreover, FL has been used in the Internet of Things (IoT), wireless networks, mobile devices, and autonomous vehicles for its excellent potential in privacy security [4–8].

Unfortunately, the distribution of local data stored in different clients varies greatly, and FedAvg performs unwise when meeting none independent and identically distributed (non-IID) data. In particular, generalization errors of the global model increase significantly with the data's statistical diversity increasing [9, 10]. To address this problem, personalized FL based on multi-task learning [11] and personalization layers [12], and local customization [13–17] have been proposed. In particular, local customization based methods fine-tune the local model to customize a personalized model. Fedprox [13] achieves good personalization through ℓ_2 -norm regularization. pFedMe [14] can decouple personalized model optimization from the global-model learning in a bi-level problem stylized based on Moreau envelopes. Per-FedAvg [16] sets up an initial meta-model that can be updated effectively after one more gradient descent step. FedAMP and HeurFedAMP [15] utilize the attentive message passing to facilitate more collaboration with similar customers. pFedGP [17] is proposed as a solution to PFL based on Gaussian processes with deep kernel learning.

Xiaofeng Liu and Qing Wang are with School of Electrical and Information Engineering, Tianjin University, Tianjin, China (e-mail: xiaofengliull@tju.edu.cn, wangqq@tju.edu.cn)

Yinchuan Li and Yunfeng Shao are with Huawei Noah's Ark Lab, Beijing, China (e-mail: liyinchuan@huawei.com, shaoyunfeng@huawei.com)

* Equal Contribution. This work was completed while Xiaofeng Liu was a member of the Huawei Noah's Ark Lab for Advanced Study.

Corresponding author: Qing Wang.

The proposed sFedHP is a local customization based personalized FL method, so we compare the performance of sFedHP with other local customization based personalized FL methods, including [13–17].

Moreover, frequent communication between clients and the server is usually required in FL to ensure convergence performance, which suffers high latency and limited bandwidth. Therefore, effective communication methods, such as sparse optimizers [18–20], quantization methods [21], ternary compression [22], and predictive coding [23] have emerged in recent years to address the limitations on communications in FL networks. sFedHP achieve sparse based on sparse constraints. since above communication-efficient methods can be combined with sFedHP, we haven't compared with them in this work.

In this paper, we propose a sparse FL with hierarchical personalized models (sFedHP) by using a hierarchical proximal mapping based on ℓ_2 -norm and a sparse constraint based on approximated ℓ_1 -norm. sFedHP decouples optimizing personalized client and edge models from learning the global model in a tri-level scheme.

Our main contributions in this paper are summarized as follows:

(1) We formulate a new tri-level optimization problem designed for sparse FL with hierarchical personalization models (sFedHP) by using a hierarchical proximal mapping based on ℓ_2 -norm and a sparse constraint based on approximated ℓ_1 -norm. The approximated ℓ_1 -norm constraints in sFedHP can greatly reduce communication cost by generating sparse models. The hierarchical proximal mapping based on ℓ_2 -norm encourages clients and edge servers to pursue their personalized models in different directions but not stay far from the reference model, significantly improving the global model performance on non-IID data. In addition, the tri-level scheme decouples the process of optimizing personalized client and edge models from learning the global model. Hence, different from the standard FL algorithm (e.g. FedAvg [3]), sFedHP can parallelly optimize the personalized models with low complexity.

(2) We present the convergence analysis of sFedHP by exploiting the convexity-preserving and smoothness-enabled properties of the loss function, which characterizes two notorious issues (client-sampling and client-drift errors) in FL [24]. With carefully tuned hyperparameters, theoretical analysis shows that sFedHP's convergence rate is state-of-the-art with linear speedup.

(3) We empirically evaluate the performance of sFedHP using different datasets that capture the statistical diversity of clients' data. We show that sFedHP obtained the state-of-the-art performance while greatly reducing the number of parameters by 80%. Moreover, sFedHP with non-sparse version outperforms FedAvg, the hierarchical FedAvg [25], and other local customization based personalized FL methods [13, 15–17] in terms of global model.

The remainder of the paper is organized as follow. The problem formulation and algorithm are formulated in Section 2. Section 3 shows the convergence analysis with some important Lemmas and Theorems. Section 4 presents the experimental results, followed by some analysis. Finally, conclusion and discussions are given in Section 5.

Other Notations: $\|\cdot\|_1$ and $\|\cdot\|_2$ denotes the ℓ_1 -norm and ℓ_2 -norm respectively; lower case and boldface lower case letters represent scalars and vectors, respectively; $\mathbb{E}(\cdot)$ denotes expectation function; $\mathcal{O}(\cdot)$ denotes same-order infinitesimal function.

2 Sparse Federated Learning with Hierarchical Personalized Models (sFedHP)

2.1 sFedHP: Problem Formulation

Consider a client-edge-cloud framework with one cloud server, N edge servers and NJ clients, i.e., each edge server collects data from J clients as showed in Fig. 1. In sFedHP, we aims to find a *sparse global-model* \mathbf{w} based on local *sparse personalized models* $\boldsymbol{\theta}_{i,j}$, $i = 1, \dots, N$, $j = 1, \dots, J$, which can greatly reduce the model size and communication costs, by minimizing

$$\text{sFedHP: } \min_{\mathbf{w} \in \mathbb{R}^d} \left\{ F(\mathbf{w}) \triangleq \frac{1}{N} \sum_{i=1}^N F_i(\mathbf{w}) \right\}, \quad (1)$$

with

$$F_i(\mathbf{w}) \triangleq \frac{1}{J} \sum_{j=1}^J F_{i,j}(\mathbf{w}), \quad (2)$$

$$F_{i,j}(\mathbf{w}) = \min_{\boldsymbol{\varphi}_{i,j}, \boldsymbol{\theta}_{i,j} \in \mathbb{R}^d} \ell_{i,j}(\boldsymbol{\theta}_{i,j}) + \frac{\lambda_1}{2} \|\boldsymbol{\theta}_{i,j} - \boldsymbol{\varphi}_{i,j}\|_2^2 + \gamma_1 \phi_\rho(\boldsymbol{\theta}_{i,j}) + \frac{\lambda_2}{2} \|\boldsymbol{\varphi}_{i,j} - \mathbf{w}\|_2^2 + \gamma_2 \phi_\rho(\mathbf{w}) \quad (3)$$

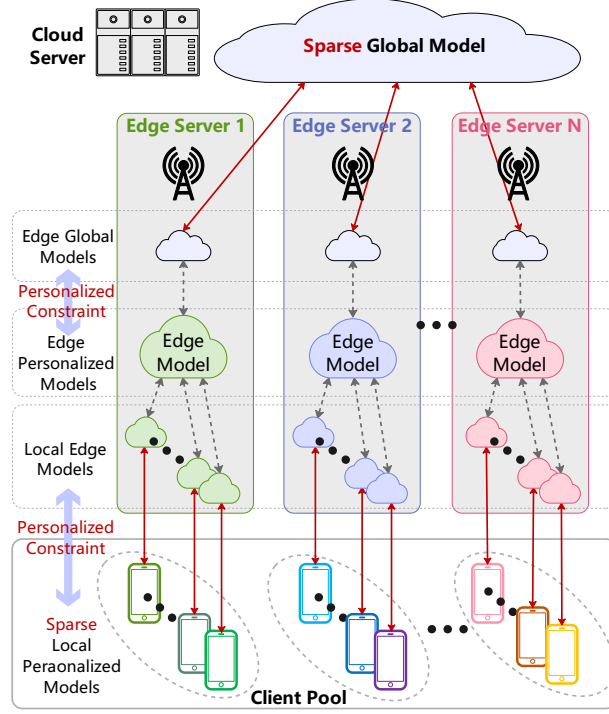


Figure 1: Sparse client-edge-cloud FL with hierarchical personalized models.

where $\ell_{i,j}(\cdot) : \mathbb{R}^d \rightarrow \mathbb{R}$ denotes the expected loss over the data distribution of the i -th edge server and the j -th client; λ_1 and λ_2 denoting regularization parameters that control the strength of \mathbf{w} to the personalized model; $\varphi_{i,j}$ is the local edge model of the i -th edge server and the j -th client; γ_1 and γ_2 denoting weight factors that control the sparsity level; and $\phi_\rho(\mathbf{x})$ being a twice continuously differentiable approximation for $\|\mathbf{x}\|_1$ [26], which is given by

$$\phi_\rho(\mathbf{x}) = \rho \sum_{n=1}^d \log \cosh \left(\frac{x_n}{\rho} \right), \quad (4)$$

where x_n denotes the n -th element in \mathbf{x} and ρ is a weight parameter, which controls the smoothing level. Note that we use $\phi_\rho(\cdot)$ instead of $\|\cdot\|_1$ to exploit the sparsity in \mathbf{w} and $\boldsymbol{\theta}$, since it makes the loss function continuously differentiable, allowing us to analyze the convergence of sFedHP through gradient and backpropagation in the network.

Overall, the idea behind (3) is that we want to find a sparse global-model \mathbf{w} , while allowing clients to find their own models $\boldsymbol{\theta}_{i,j}$ with different directions within a proper distance from the ‘‘reference point’’ \mathbf{w} . It is noteworthy that we do not directly impose sparse constraints on $\varphi_{i,j}$ in (3) because after both \mathbf{w} and $\boldsymbol{\theta}_{i,j}$ are sparse, we observe that $\varphi_{i,j}$ is already sparse, and eliminating the constraints can reduce the computational burden.

Our sFedHP minimizes the loss function in a tri-level manner. In the first level, \mathbf{w} is determined by utilizing the sparse model aggregation from multiple edges. In the second level, the edge personalized model φ_i and the local edge model $\varphi_{i,j}$ are determined by minimizing (3) w.r.t. the client models of the i -th edge server

$$\begin{aligned} \hat{\varphi}_i(\mathbf{w}) &= \frac{1}{J} \sum_{i=1}^J \hat{\varphi}_{ij}(\mathbf{w}), \\ \hat{\varphi}_{ij}(\mathbf{w}) &= \arg \min_{\varphi_{ij} \in \mathbb{R}^d} \frac{\lambda_1}{2} \left\| \hat{\boldsymbol{\theta}}_{i,j} - \varphi_{ij} \right\|_2^2 + \frac{\lambda_2}{2} \left\| \varphi_{ij} - \mathbf{w} \right\|_2^2, \end{aligned} \quad (5)$$

where the optimal local personalized model $\hat{\boldsymbol{\theta}}_{i,j}$ is determined by minimizing (3) w.r.t. the data distribution of the i -th edge server and j -th client in the third level as the following

$$\hat{\boldsymbol{\theta}}_{i,j}(\varphi_{i,j}) = \arg \min_{\boldsymbol{\theta}_{i,j} \in \mathbb{R}^d} L_{i,j}(\boldsymbol{\theta}_{i,j}) + \frac{\lambda_1}{2} \left\| \boldsymbol{\theta}_{i,j} - \varphi_{i,j} \right\|_2^2, \quad (6)$$

where $L_{i,j}(\boldsymbol{\theta}_{i,j}) \triangleq \ell_{i,j}(\boldsymbol{\theta}_{i,j}) + \gamma_1 \phi_\rho(\boldsymbol{\theta}_{i,j})$. In the next section, we will present the details of solving this tri-level problem.

2.2 sFedHP : Algorithm

We propose the sFedHP algorithm, and the pseudo-code is presented in Algorithm 1. At t -th communication round, the cloud server broadcasts the global model \mathbf{w}^t to all edge servers. Then, the edge servers with their clients complete R rounds of iterative training and upload the edge global model \mathbf{w}_i^t to aggregate a new global model \mathbf{w}^{t+1} . Moreover, similarly with [14,24], an additional parameter β is used for global-model update to improve the convergence performance. Note that communication between the clients and edge servers is more efficient than between the clients and the cloud server. The latter's communication is high cost and latency because the distance is relatively long.

At the first level, once edge personalized models are updated, the edge global models can be updated by stochastic gradient descent as follows

$$\begin{aligned}\mathbf{w}_i^{t,r+1} &= \mathbf{w}_i^{t,r} - \eta_1 \nabla F_i(\mathbf{w}_i^{t,r}), \\ &= \mathbf{w}_i^{t,r} - \eta_1 [\lambda_2(\mathbf{w}_i^{t,r} - \check{\varphi}_i^{t,r+1}) + \gamma_2 \nabla \phi_\rho(\mathbf{w}_i^{t,r})],\end{aligned}\quad (7)$$

where η_1 is a learning rate and $\mathbf{w}_i^{t,r}$ is the edge global model of i -th edge server at the global round t and edge round r .

At the second level, after clients' local personalized models are updated, the local edge models are determined by

$$\check{\varphi}_i^{t,r+1} = (\lambda_1 \check{\theta}_{i,j}^{t,r} + \lambda_2 \mathbf{w}_i^{t,r}) / (\lambda_1 + \lambda_2), \quad (8)$$

where $\check{\varphi}_i = \frac{1}{J} \sum_{i=1}^J \check{\varphi}_{i,j}$ is the current edge personalized model of the i -th edge server.

At the third level, the local personalized model $\hat{\theta}_{i,j}$ of the i -th edge server and the j -th client is determined by solving (6), whose parameters are sparse and can reduce the communication load between clients and edge servers. Note that (6) can be easily solved by many first-order approaches, for example, Nesterov's accelerated gradient descent, based on the gradient. However, calculate the exactly $\nabla \ell_{i,j}(\boldsymbol{\theta}_{i,j})$ requires the distribution of $Z_{i,j}$, we hence use the unbiased estimate by sampling a mini-batch of data $\mathcal{D}_{i,j}$,

$$\nabla \check{\ell}_{i,j}(\boldsymbol{\theta}_{i,j}, \mathcal{D}_{i,j}) = \frac{1}{|\mathcal{D}_{i,j}|} \sum_{Z_{i,j} \in \mathcal{D}_{i,j}} \nabla \ell_{i,j}(\boldsymbol{\theta}_{i,j}, Z_{i,j}). \quad (9)$$

Thus, we solve the following minimization problem instead of solving (6) to obtain an approximated local personalized model

$$\check{\theta}_{i,j}(\varphi_{i,j}^{t,r}) = \arg \min_{\boldsymbol{\theta}_{i,j} \in \mathbb{R}^d} H(\boldsymbol{\theta}; \varphi_{i,j}^{t,r}, \mathcal{D}_{i,j}), \quad (10)$$

where $H(\boldsymbol{\theta}_{i,j}; \varphi_{i,j}^{t,r}, \mathcal{D}_{i,j}) = \check{\ell}_{i,j}(\boldsymbol{\theta}_{i,j}, \mathcal{D}_{i,j}) + \gamma_1 \phi_\rho(\boldsymbol{\theta}_{i,j}) + \frac{\lambda_1}{2} \|\boldsymbol{\theta}_{i,j} - \varphi_{i,j}^{t,r}\|_2^2$. Similarly, (10) can be solved by Nesterov's accelerated gradient descent, we let the iteration goes until the condition

$$\|\nabla H(\check{\theta}_{i,j}; \varphi_{i,j}^{t,r}, \mathcal{D}_{i,j})\|_2^2 \leq \nu, \quad (11)$$

is reached, where ν is an accuracy level.

3 Convergence Analysis

3.1 Convergence Theorems

We first present some useful assumptions, which are widely used in FL gradient calculation and convergence analysis [14, 16, 24, 27]. Then, Theorem 1 shows the smoothness and strong convexity properties of objective function in sFedHP. Finally, the convergence of sFedHP for strong convex and nonconvex cases are presented in Theorems 2 and 3 respectively.

Assumption 1. (Strong convexity and smoothness) Assume that $\ell(\mathbf{w}) : \mathbb{R}^d \rightarrow \mathbb{R}$ is (a) μ -strongly convex or (b) nonconvex and L -smooth on \mathbb{R}^d , then we respectively have the following inequalities

$$\begin{aligned}(a) \quad &\ell(\mathbf{w}) \geq \ell(\bar{\mathbf{w}}) + \langle \nabla \ell(\bar{\mathbf{w}}), \mathbf{w} - \bar{\mathbf{w}} \rangle + \frac{\mu}{2} \|\mathbf{w} - \bar{\mathbf{w}}\|_2^2, \\ (b) \quad &\|\nabla \ell(\mathbf{w}) - \nabla \ell(\bar{\mathbf{w}})\|_2 \leq L \|\mathbf{w} - \bar{\mathbf{w}}\|_2.\end{aligned}$$

Algorithm 1 sFedHP: Sparse Federated Learning with Hierarchical Personalization Models Algorithm

Input: hyperparameters in (3) $\{\lambda_1, \lambda_2, \gamma_1, \gamma_2, \rho\}$
 communication rounds $\{T, R\}$
 init parameters \mathbf{w}^0
 client learning rate η_1 , server learning rate η_2

Cloud server executes:

for $t = 0, 1, \dots, T - 1$ **do**

for $i = 1, 2, \dots, N$ **in parallel do**

$\mathbf{w}_i^{t+1} \leftarrow \text{EdgeUpdate}(i, \mathbf{w}^t)$

$\mathcal{S}^t \leftarrow (\text{random set of } S \text{ edge servers})$

$\mathbf{w}^{t+1} = (1 - \beta)\mathbf{w}^t + \frac{\beta}{S} \sum_{i \in \mathcal{S}^t} \mathbf{w}_i^{t+1}$

EdgeUpdate(i, \mathbf{w}^t):

$\varphi_i^{t,0} = \mathbf{w}_i^{t,0} = \mathbf{w}^t$

for $r = 0, 1, \dots, R - 1$ **do**

for $j = 1, \dots, J$ **in parallel do**

 Update the local personalized model $\theta_{i,j}$:
 $\mathcal{D}_{i,j} \leftarrow (\text{sample a mini-batch with size } |\mathcal{D}|)$
 $\check{\theta}_{i,j}^{t,r}(\varphi_i^{t,r}) = \arg \min_{\theta_{i,j} \in \mathbb{R}^d} H(\theta_{i,j}; \varphi_i^{t,r}, \mathcal{D}_{i,j})$

 Update the local edge model $\varphi_{i,j}$ according to (5):
 $\check{\varphi}_{i,j}^{t,r+1} = (\lambda_1 \check{\theta}_{i,j}^{t,r} + \lambda_2 \mathbf{w}_i^{t,r}) / (\lambda_1 + \lambda_2)$

 Update the edge personalized model φ_i :
 $\varphi_i^{t,r+1} = \frac{1}{J} \sum_{j=1}^J \check{\varphi}_{i,j}^{t,r+1}$

$\mathbf{w}_i^{t,r+1} = \mathbf{w}_i^{t,r} - \eta_1 [\lambda_2 (\mathbf{w}_i^{t,r} - \varphi_i^{t,r+1}) + \gamma_2 \nabla \phi_\rho(\mathbf{w}_i^{t,r})]$

 Return $\mathbf{w}_i^{t+1} = \mathbf{w}_i^{t,R}$ to the cloud server

Assumption 2. (Bounded variance) The variance of stochastic gradients (sampling noise) in each client is bounded by

$$\mathbb{E}_{\mathcal{Z}} \left[\left\| \nabla \check{\ell}_{i,j}(\mathbf{w}; Z_{i,j}) - \nabla \ell_{i,j}(\mathbf{w}) \right\|_2^2 \right] \leq \gamma_\ell^2,$$

where $Z_{i,j}$ is the training data randomly drawn from the distribution of client i and edge server j .

Assumption 3. (Bounded diversity) The diversity of client's data distribution is bounded by

$$\frac{1}{NJ} \sum_{i,j=1}^{N,J} \left\| \nabla \ell_{i,j}(\mathbf{w}) - \nabla \ell(\mathbf{w}) \right\|_2^2 \leq \sigma_\ell^2.$$

Then, we have the following Theorem 1 under Assumptions 1-3, which presents the smoothness and strong convexity properties of $F_{i,j}(\mathbf{w})$.

Theorem 1. If $\ell_{i,j}$ is convex or nonconvex with L -Lipschitz $\nabla \ell_{i,j}$, then $F_{i,j}$ is L_F -smooth with $L_F = \lambda_2 + \frac{\gamma_2}{\rho}$ (with the condition that $\lambda_2 > 4L + \frac{4\gamma_1}{\rho}$ for nonconvex L -smooth $\ell_{i,j}$) and if $\ell_{i,j}$ is μ -strongly convex, then $F_{i,j}$ is μ_F -strongly convex with $\mu_F = \frac{\lambda_1 \lambda_2 \mu}{\lambda_1 \mu + \lambda_2 \mu + \lambda_1 \lambda_2}$.

For unique solution \mathbf{w}^* to sFedHP, we have the following convergence theorems, Theorems 2 and 3, based on Assumptions 1-3 and Theorem 1.

Theorem 2. (Strongly convex sFedHP's convergence). Let Assumptions 1(a) and 2 hold, there exists an $\check{\eta} \leq \min[\frac{1}{\mu_F}, \frac{1}{3L_F(3+128L_F/(\mu_F\beta))}]$, such that

$$(a) \mathbb{E} [F(\mathbf{w}^T) - F(\mathbf{w}^*)] \leq \frac{\Delta_0}{\check{\eta}T} + M_1 + \check{\eta}M_2,$$

$$(b) \frac{1}{NJ} \sum_{i,j=1}^{N,J} \mathbb{E} \left[\left\| \check{\ell}_{i,j}^T(\mathbf{w}^T) - \mathbf{w}^* \right\|_2^2 \right] \leq \mathcal{O} \left(\frac{L_F + \lambda^2}{\lambda^2 \mu_F} \right) \mathbb{E} [F(\mathbf{w}_T) - F^*] + \mathcal{O}(D_1),$$

where $\Delta_0 \triangleq \|\mathbf{w}_0 - \mathbf{w}^*\|^2$, $M_1 = \frac{8\delta^2 \bar{\lambda}^2}{\mu_F}$, $M_2 = 6(1 + 64\frac{L_F}{\mu_F \beta})\sigma_{F,1}^2 + \frac{128L_F \delta^2 \bar{\lambda}^2}{\mu_F \beta}$, $\lambda \triangleq \frac{\lambda_1 \lambda_2}{\sqrt{\lambda_1^2 + \lambda_2^2}}$, $\bar{\lambda} \triangleq \frac{\lambda_1 \lambda_2}{\lambda_1 + \lambda_2}$ and

$D_1 = \sigma_{F,1}^2 / \lambda^2 + \gamma_2^2 d_s^2 / \bar{\lambda}^2 + \delta^2$ with $\sigma_{F,1}^2 \triangleq \frac{1}{NJ} \sum_{i,j=1}^{N,J} \|\nabla F_{i,j}(\mathbf{w}^*)\|_2^2$, δ being the sampling noise and d_s denoting the number of non-zero elements in the global-model \mathbf{w} .

Theorem 3. (Nonconvex and smooth $sF\ominus dHP$'s convergence). Let Assumptions 1(b), 2 and 3 hold, there exists an $\check{\eta} \leq \min[\frac{1}{588L_F\lambda^2}, \frac{\beta}{2L_F}]$ with $\lambda \leq \sqrt{16(L + \frac{\gamma_1}{\rho})^2 + 1}$, such that

$$(a) \frac{1}{T} \sum_{t=0}^{T-1} \mathbb{E} \left[\|\nabla F(\mathbf{w}^t)\|_2^2 \right] \leq 4 \left(\frac{\Delta_F}{\check{\eta}T} + G_1 + \check{\eta}^1 G_2 \right)$$

$$(b) \frac{1}{T} \sum_{t=0}^{T-1} \frac{1}{NJ} \sum_{i,j=1}^N \mathbb{E} \left[\|\check{\theta}_{i,j}(\mathbf{w}^t) - \mathbf{w}^t\|_2^2 \right] \leq \frac{1}{T} \sum_{t=0}^{T-1} \mathbb{E} \left[\|\nabla F(\mathbf{w}^t)\|_2^2 \right] + \mathcal{O}(D_2),$$

where $\Delta_F \triangleq F(\mathbf{w}_0) - F^*$, $G_1 = 3\beta\bar{\lambda}^2\delta^2$, $G_2 = \frac{3L_F(49R\sigma_{F,2}^2 + 16\delta^2\bar{\lambda}^2)}{R}$ and $D_2 = \sigma_{F,2}^2/\lambda^2 + \gamma_2^2 d_s^2/\bar{\lambda}^2 + \delta^2$ with $\sigma_{F,2}^2 \triangleq \frac{\lambda^2}{\lambda^2 - 16(L + \frac{\gamma_1}{\rho})^2} \sigma_\ell^2$.

Remark 1. Theorems 2(a) and 3(a) show the convergence results of the global-model. Δ_0 and Δ_F denote the initial error which can be reduced linearly. Theorem 2(b) and 3(b) show that the convergence of personalized client models in average to a ball of center \mathbf{w}^* and radius $\mathcal{O}(D_1)$ and $\mathcal{O}(D_2)$, respectively, for μ -strongly convex and nonconvex. Note that, our $sF\ominus dHP$ obtain sparsity with a convergence speed cost $\mathcal{O}(\gamma_2^2 d_s^2/\bar{\lambda}^2)$, the experimental results show that a good sparsity can be obtained by only using a tiny γ_2 , yields $\gamma_2^2 d_s^2/\bar{\lambda}^2 \ll \{\sigma_{F,1}^2/\lambda^2, \sigma_{F,2}^2/\lambda^2\}$, i.e., the convergence speed cost of the sparse constraints can be omitted. The proofs of Theorems 1, Theorems 2 and 3 are presented in Appendix.

3.2 Some Important Lemmas

In this subsection, we present some important lemmas, which are well used in the proof of Theorems 2 and 3, to help better understand the conclusion of the these convergence theorem.

We re-write the local update in (7) as follow:

$$\mathbf{w}_i^{t,r+1} = \mathbf{w}_i^{t,r} - \eta_1 \lambda_2 \underbrace{\left[\left(\mathbf{w}_i^{t,r} - \check{\varphi}_i^{t,r+1} \right) + \gamma_2 \nabla \phi_\rho(\mathbf{w}_i^{t,r}) \right]}_{\triangleq g_i^{t,r}},$$

which implies

$$\eta_1 \sum_{r=0}^{R-1} g_i^{t,r} = \sum_{r=0}^{R-1} \left(\mathbf{w}_i^{t,r} - \mathbf{w}_i^{t,r+1} \right) = \mathbf{w}^t - \mathbf{w}_i^{t,R},$$

where $g_i^{t,r}$ can be interpreted as the biased estimate of $\nabla F_i(\mathbf{w}_i^{t,r})$ since $\mathbb{E}(g_i^{t,r}) \neq \nabla F_i(\mathbf{w}_i^{t,r})$. Then, we re-write the global update as

$$\mathbf{w}^{t+1} = (1-\beta)\mathbf{w}^t + \frac{\beta}{S} \sum_{i \in \mathcal{S}^t} \mathbf{w}_i^{t,R} = \mathbf{w}^t - \check{\eta} \frac{1}{SR} \sum_{i \in \mathcal{S}^t} \sum_{r=0}^{R-1} g_i^{t,r},$$

where $\check{\eta} \triangleq \eta_1 \beta R$ and $g^t \triangleq \frac{1}{SR} \sum_{i \in \mathcal{S}^t} \sum_{r=0}^{R-1} g_i^{t,r}$ can be respectively considered as the step size and approximate stochastic gradient of the global update, which cause drift error in one-step update of the global model formulated in Lemma 1.

Lemma 1 (One-step global update). Let Assumption 1(b) holds. We have

$$\begin{aligned} & \mathbb{E} \left[\|\mathbf{w}^{t+1} - \mathbf{w}^*\|_2^2 \right] \\ & \leq \mathbb{E} \left[\|\mathbf{w}^t - \mathbf{w}^*\|_2^2 \right] - \check{\eta} (2 - 6L_F \check{\eta}) \mathbb{E} [F(\mathbf{w}^t) - F(\mathbf{w}^*)] \\ & \quad + \frac{\check{\eta} (3\check{\eta} + 1/\mu_F)}{NR} \sum_{i,r}^{N,R} \mathbb{E} \left[\|g_i^{t,r} - \nabla F_i(\mathbf{w}^t)\|_2^2 \right] \\ & \quad + 3\check{\eta}^2 \frac{1}{NJ} \sum_{i,j=1}^{N,J} \mathbb{E} \left[\|\nabla F_{i,j}(\mathbf{w}^t) - \nabla F(\mathbf{w}^t)\|_2^2 \right], \end{aligned}$$

where $\sum_{i,r}^{N,R}$ and $\sum_{i,j}^{N,J}$ are respectively used as alternatives for $\sum_{i=1,r=0}^{N,R-1}$ and $\sum_{i,j=1}^{N,J}$.

The various parts of Lemma 1 are discussed in detail in the following Lemmas.

Lemma 2 (Bounded diversity of $\theta_{i,j}$ w.r.t. mini-batch sampling). *For the solution $\check{\theta}_{i,j}(\varphi_{i,j}^{t,r})$ to (10), we have*

$$\mathbb{E} \left[\left\| \check{\theta}_{i,j}(\varphi_{i,j}^{t,r}) - \hat{\theta}_{i,j}(\varphi_{i,j}^{t,r}) \right\|_2^2 \right] \leq \delta^2,$$

with

$$\delta^2 \triangleq \begin{cases} \frac{2}{(\lambda_1 + \mu)^2} \left(\frac{\gamma_1^2}{|\mathcal{D}|} + \nu \right), & \text{if A.1(a) holds;} \\ \frac{2}{(\lambda_1 - L - \frac{\gamma_1}{\rho})^2} \left(\frac{\gamma_1^2}{|\mathcal{D}|} + \nu \right), & \text{if A.1(b) holds.} \end{cases}$$

where $\lambda_1 > L + \gamma_1/\rho$ is required for A.1(b) case.

Lemma 3 (Bounded edge server drift error). *If $\check{\eta} \leq \frac{\beta}{2L_F}$, we have*

$$\frac{1}{NR} \sum_{i,r=1}^{N,R} \mathbb{E} \left[\|g_i^{t,r} - \nabla F_i(\mathbf{w}^t)\|_2^2 \right] \leq 2\bar{\lambda}^2 \delta^2 + \frac{16L_F \check{\eta}}{\beta} \left(3 \frac{1}{NJ} \sum_{i,j=1}^{NJ} \mathbb{E} \left[\|\nabla F_{i,j}(\mathbf{w}^t)\|_2^2 \right] + \frac{2\bar{\lambda}^2 \delta^2}{R} \right),$$

where $g_i^{t,r} = \lambda_2 \left[\left(\mathbf{w}_i^{t,r} - \check{\varphi}_i^{t,r+1} \right) + \gamma_2 \nabla \phi_\rho(\mathbf{w}_i^{t,r}) \right]$ and $\bar{\lambda} = \frac{\lambda_1 \lambda_2}{\lambda_1 + \lambda_2}$.

Lemma 4 (Bounded diversity of F_i w.r.t. distributed training). *Let \mathbf{w}^* denote the optimal solution for (1), we have*

$$\frac{1}{NJ} \sum_{i=1,j=1}^{N,J} \|\nabla F_{i,j}(\mathbf{w}) - \nabla F(\mathbf{w})\|_2^2 \leq \begin{cases} 4L_F(F(\mathbf{w}) - F(\mathbf{w}^*)) + 2\sigma_{F,1}^2, & \text{if A.1(a) holds;} \\ \frac{16(L + \frac{\gamma_1}{\rho})^2}{\lambda^2 - 16(L + \frac{\gamma_1}{\rho})^2} \|\nabla F(\mathbf{w})\|_2^2 + 2\sigma_{F,2}^2, & \text{if A.1(b) holds.} \end{cases}$$

where $\lambda > 4(L + \gamma_1/\rho)$ is required for A.1(b) case, $\sigma_{F,1}^2 \triangleq \frac{1}{NJ} \sum_{i,j=1}^{N,J} \|\nabla F_{i,j}(\mathbf{w}^*)\|_2^2$, $\lambda = \frac{\lambda_1 \lambda_2}{\sqrt{\lambda_1^2 + \lambda_2^2}}$ and $\sigma_{F,2}^2 \triangleq \frac{\lambda^2}{\lambda^2 - 16(L + \frac{\gamma_1}{\rho})^2} \sigma_\ell^2$.

Remark 2. Lemma 2 and Lemma 3 show the diversity and drift errors caused by mini-batch training strategy are bounded. While, Lemma 4 shows the effect w.r.t. distributed training is bounded. By combining Lemma 1-4, we can get the recurrence relation between $\mathbf{w}^t - \mathbf{w}^*$ and $F(\mathbf{w}^t) - F(\mathbf{w}^*)$ in Theorems 2 and 3. The proofs of Lemma 1-4 are presented in Appendix.

4 Experimental Results

4.1 Experimental Setting

This section presents the empirical performance of sFedHP with heterogeneous and non-i.i.d data. We evaluate our method based on MNIST [28] by using the heterogeneous setting strategy in [14] for $N = 20$ clients. Each client occupies unique local data with different data size and only has 2 of the 10 labels. As for our client-edge-cloud framework, we set 2 edge servers in our experiments and each edge server manage 10 clients. Similarly with [14], in each round of local training, the client uses $K = 5$ gradient-based iterations to obtain an approximated optimal local model, i.e., solve (10) in sFedHP.

An ℓ_2 -regularized multinomial logistic regression model (MLR) is used for μ -strong convex situation, while a deep neural network (DNN) with two hidden layers is used for nonconvex situation. In our experiments, $\frac{3}{4}$ datasets are for training and the others are for testing. All experiments were conducted on a NVIDIA Quadro RTX 6000 environment, and the code based on PyTorch is available online.

4.2 Effect of hyperparameters

We first empirically study the effect of different hyperparameters in sFedHP on MNIST dataset.

Effects of λ : According to Fig. 2, properly increasing λ can effectively improve the test accuracy and convergence rate for sFedHP. And we find that an oversize λ_1 and λ_2 may cause gradient explosion.

Effects of R : In sFedHP, R denotes the edge local epochs, larger R requires more communication round between clients and edge servers.

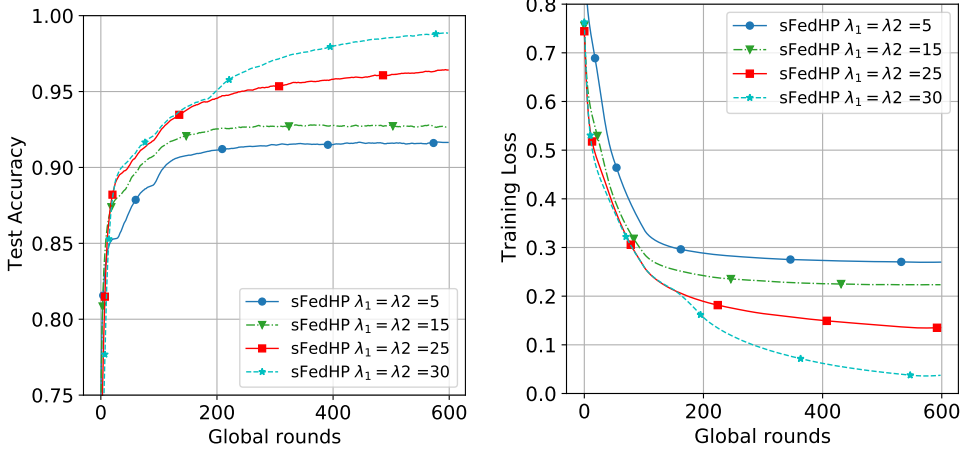


Figure 2: Effect of λ on the convergence of sFedHP on MNIST ($\rho = 6 \times 10^{-5}$, $\gamma_1 = \gamma_2 = 0.008$, $R = 20$, $K = 5$, $\beta = 1$).

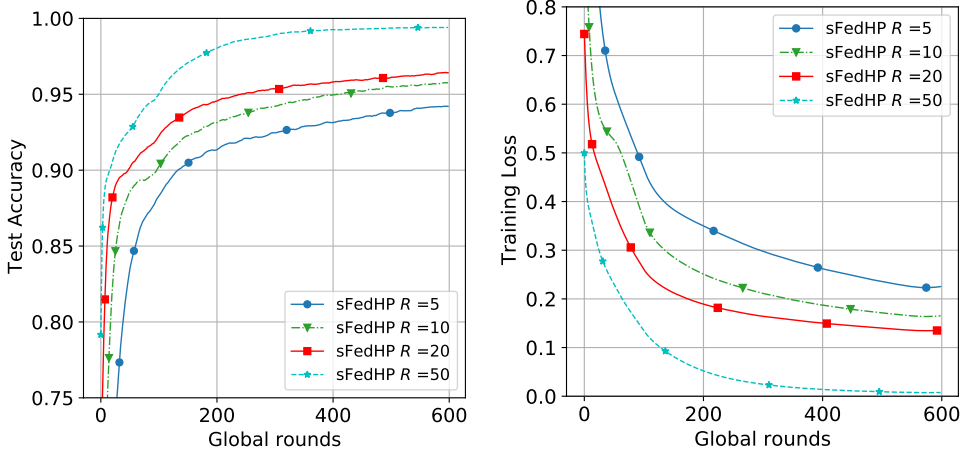


Figure 3: Effect of R on the convergence of sFedHP on MNIST ($\rho = 6 \times 10^{-5}$, $\gamma_1 = \gamma_2 = 0.008$, $\lambda_1 = \lambda_2 = 25$, $K = 5$, $\beta = 1$).

Effects of β : Fig. 4 shows the experiment results related with β . We find that a larger β converges faster, but we don't want it to be greater than 1 because it may cause instability.

Effects of γ : Fig. 5 shows the relationship of γ with the model sparsity and the convergence speed, we can see that increasing γ will reduce the communication speed and global accuracy.

4.3 Performance Comparison

We compare the global-model between sFedHP, pFedMe [14] and hierarchical FedAvg [25] on μ -strongly convex and nonconvex situations. We use both sparsity and non-sparsity settings for sFedHP. In the sparsity setting, we set $\gamma_1 = \gamma_2 = 0.001$ at the beginning, while set γ_1 and γ_2 to a tiny number respectively when the client model sparsity is lower than 0.2 and after training 100 global rounds. Since according to our theoretical results, a tiny γ_1, γ_2 can reduce the convergence cost. In non-sparsity setting, we set $\gamma_1 = \gamma_2 = 0$.

We test both sFedHP and hierarchical FedAvg in a client-edge-cloud framework, while pFedMe in a cloud-client framework, to evaluate the performance advantage of hierarchical personalization models. To balance the difference, in each global iteration, only 10 client models are used to generate the global-model in sFedHP, FedAvg and pFedMe.

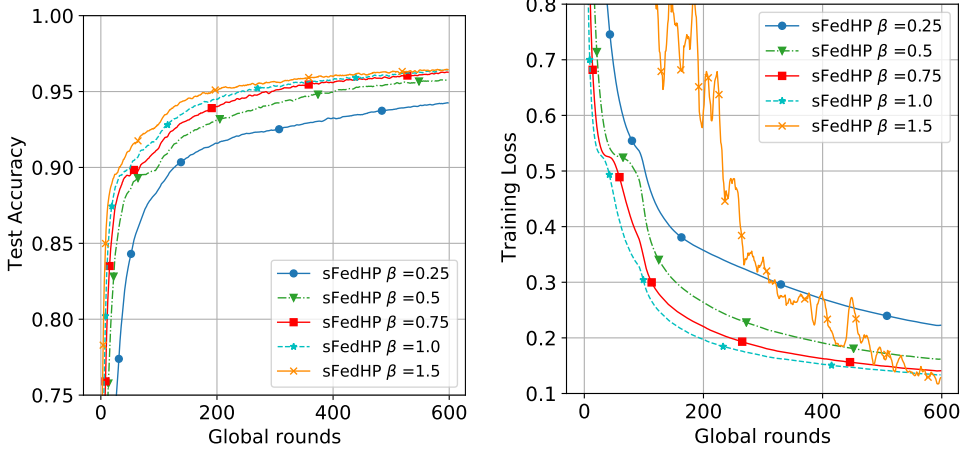


Figure 4: Effect of γ on the convergence of sFedHP on MNIST ($\rho = 6 \times 10^{-5}$, $R = 20$, $\lambda_1 = \lambda_2 = 25$, $K = 5$, $\gamma_1 = \gamma_2 = 0.008$).

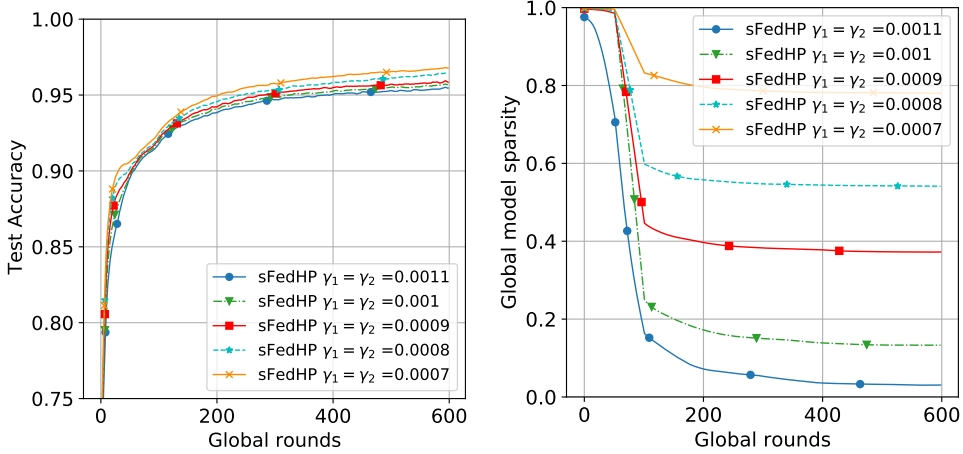


Figure 5: Effect of γ on the convergence of sFedHP on MNIST ($\rho = 6 \times 10^{-5}$, $R = 20$, $\lambda_1 = \lambda_2 = 25$, $K = 5$, $\beta = 1$).

Fig. 6 shows the performance of sFedHP, hierarchical FedAvg and pFedMe in μ -strongly convex situation. Since the MLR model is already lightweight enough, we set $\gamma_1 = \gamma_2 = 0$ for sFedHP. In Fig. 6, we can see that both sFedHP and pFedMe perform better than hierarchical FedAvg, while sFedHP obtain higher test accuracy and convergence speed, which shows that the hierarchical personalization scheme is more suitable for solving statistical diversity problem.

Fig. 7 shows the performance of sFedHP, hierarchical FedAvg and pFedMe in nonconvex situation. We test sparsity and non-sparsity settings for sFedHP in accuracy, model sparsity and the accumulative communication. We set 20% sparsity, the proportion of non-zero parameters, as a lower bound to preserve performance. According to Fig. 7, the proposed sFedHP can reduce the communication cost while achieve good test accuracy simultaneously. Specific, sFedHP obtain similar performance in a global model with pFedMe while reducing communication costs by 80% and obtain higher performance when using a non-sparsity setting.

Remark 3. *The accumulated communication cost in Fig. 6 is calculated based on one client in the client-cloud FL or one edge server in the client-edge-cloud FL since the client and the edge server are nearby between which low-cost communication is possible. Consider the DNN model with 79510 parameters, whose non-zero parameters are quantized in 64 bits while zero parameters are quantized in 1 bit. 79510 bits location parameters are needed to mark the positions of zero parameters in sFedHP. This section aims to demonstrate the excellent sparsity of sFedHP*

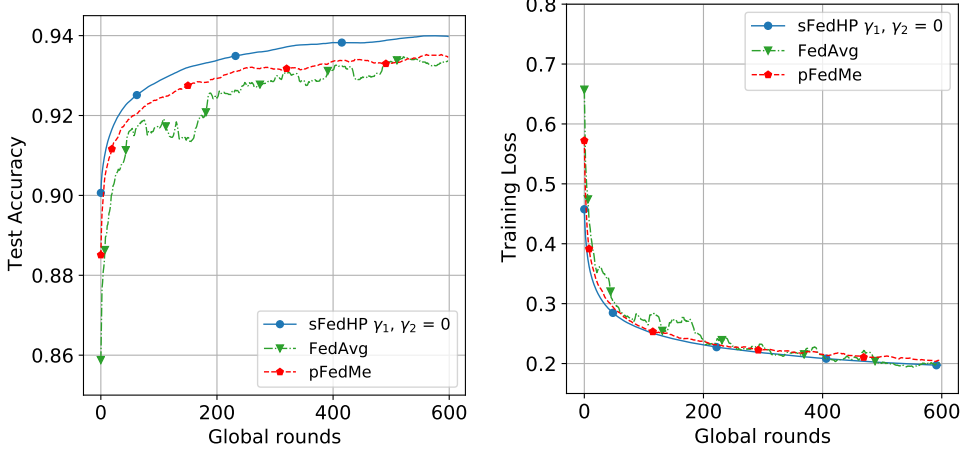


Figure 6: μ -Strongly Convex Performance comparison of sFedHP, FedAvg and pFedMe in MNIST ($\eta = 0.05, R = 20, |\mathcal{D}| = 20, \beta = 1$ for all experiments, $\lambda_1 = \lambda_2 = \lambda = 25$ for sFedHP and pFedMe)

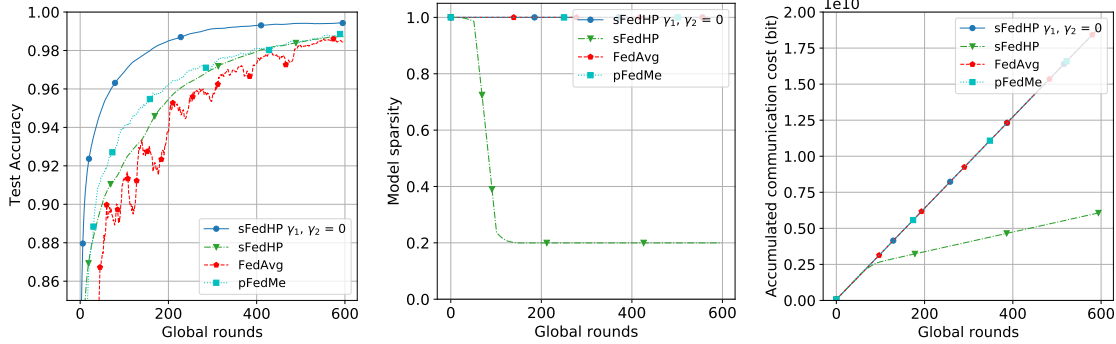


Figure 7: Nonconvex Performance comparison of sFedHP, FedAvg and pFedMe in MNIST ($\eta = 0.05, R = 20, |\mathcal{D}| = 20, \beta = 1$ for all experiments, $\lambda_1 = \lambda_2 = \lambda = 25$ for sFedHP and pFedMe)

qualitatively. We focused on analyzing the ability of sFedHP to process non-IID data under different settings. More rigorous communication cost analysis needs to cooperate with the encoding and decoding process.

In summary, sFedHP performs better than pFedMe and hierarchical FedAvg in test accuracy, convergence rate, and communication cost in μ -strongly convex and nonconvex situations. Furthermore, the hierarchical personalization scheme is more suitable for solving statistical diversity problems.

4.4 More Results

To empirically highlight the performance of the proposed method, we further compare sFedHP in non-saprsity setting with FedAvg [3], hierarchical FedAvg (HierFAVG) [25] and local customization personalized FL methods, including Fedprox [13], Per-FedAvg [16], pFedMe [14], HeurFedAMP [15], and pFedGP [17] based on MNIST [28], Fashion-MNIST (FMNIST) [29] and CIFAR-10 [30] datasets. For non-i.i.d. setups, we follow the strategy in [14] for $N = 20$ clients and assign each client a unique local data with only 5 out of 10 labels. For client-edge-cloud framework, we set 4 edge servers and each edge server manage 5 clients. All 20 clients are selected to generate the global model in following experiments.

Furthermore, we use two different dataset split settings to validate the performance of the above algorithms. In Setting 1, we used 200, 200, 100 training samples and 800, 800, 400 test samples in each class for MNIST, FMNIST and CIFAR-10 datasets respectively. In Setting 2, 900, 900, 450 training samples and 300, 300, 150 test samples are applied on MNIST, FMNIST and CIFAR-10 datasets for each class. We use the DNN model in Section 4.1 for MNIST/FMNIST

Table 1: Results on MNIST, FMNIST, CIFAR-10 and CIFAR-100. Best results are bolded.

Dataset	Method	Setting 1 (%)	Setting 2 (%)
MNIST	FedAvg [3]	91.63 \pm 0.12	94.31 \pm 0.08
	HierFAVG [25]	93.22 \pm 0.03	95.05 \pm 0.07
	Fedprox [13]	93.43 \pm 0.15	90.04 \pm 0.08
	pFedMe [14]	89.34 \pm 0.04	93.04 \pm 0.14
	Ours	94.93 \pm 0.03	97.66 \pm 0.06
FMNIST	FedAvg [3]	79.11 \pm 0.09	84.48 \pm 0.06
	HierFAVG [25]	83.55 \pm 0.15	85.48 \pm 0.08
	Fedprox [13]	78.67 \pm 0.04	84.33 \pm 0.10
	pFedMe [14]	80.57 \pm 0.07	85.14 \pm 0.11
	Ours	85.64 \pm 0.04	89.29 \pm 0.05
CIFAR-10	FedAvg [3]	42.36 \pm 0.19	81.74 \pm 0.17
	HierFAVG [25]	52.76 \pm 0.21	87.28 \pm 0.13
	Fedprox [13]	39.10 \pm 0.23	72.98 \pm 0.35
	pFedMe [14]	58.66 \pm 0.15	90.31 \pm 0.22
	Ours	78.44 \pm 0.08	94.09 \pm 0.10

datasets and the VGG model for CIFAR-10 dataset with “[16, ‘M’, 32, ‘M’, 64 ‘M’, 128, ‘M’, 128, ‘M’]” cfg setting. Each experiment is run at least 3 times to obtain statistical reports.

An excellent global model has important implications for federated learning, which can be downloaded from the cloud server achieving rapid deployment when a new client joins. Table 1 shows the performance of each algorithm with global model. We set $|\mathcal{D}| = 20$, $T = 800$, $K = 5$, and $\eta_1 = \eta_2 = 0.05$ for all algorithms and fine-tuned other basic hyperparameters. The proposed algorithm `sFedHP` outperforms compared algorithms in the global model for all situation by more than 1% (Setting 1 on MNIST), 2% (Setting 2 on MNIST), 2% (Setting 1 on FMNIST), 3% (Setting 2 on FMNIST), 19% (Setting 1 on CIFAR-10), and 3% (Setting 2 on CIFAR-10).

More detailed results for fine-tuning hyperparameters, including methods without a global model, are present in Table 2 to 5, where E represents the number of edge servers in the hierarchical framework, and α represents the proportion of the client model that does not interact with the global model in HeurFedAMP. We find `sFedHP` outperforms all compared algorithms in the global model (GM) and achieve the state-of-art results in the personalized model (PM).

Table 2: Results of all of algorithms on On MNIST with setting 1.

Method	η_1	η_2	λ	K	E	α	Acc. (%)	
							PM	GM
Fedavg [3]	0.05	-	-	5	-	-	-	91.63
HierFAVG [25]	0.05	-	-	5	4	-	-	93.22
HeurFedAMP [15]	0.05	0.05	-	5	-	0.1	97.11	-
	0.05	0.05	-	5	-	0.5	98.55	-
Fedprox [13]	0.05	-	0.001	5	-	-	-	93.43
PerFedavg [16]	0.05	-	-	5	-	-	56.5	-
pFedMe [14]	0.05	0.05	5	5	-	-	98.8	88.83
	0.05	0.05	15	5	-	-	98.92	89.34
	0.05	0.05	20	5	-	-	98.91	89.06
	0.05	0.05	25	5	-	-	97.6	80.12
	0.05	0.05	30	5	-	-	52.07	10.41
pFedGP [17]	0.05	-	-	5	-	-	98.12	-
Ours	0.05	0.05	5	5	4	-	98.24	93.06
	0.05	0.05	15	5	4	-	96.55	91.85
	0.05	0.05	20	5	4	-	97.83	94.93
	0.05	0.05	25	5	4	-	96.63	95.39
	0.05	0.05	30	5	4	-	96.23	95.63

Table 3: Results of all of algorithms on MNIST with setting 2.

Method	η_1	η_2	λ	K	E	α	Acc. (%)	
							PM	GM
Fedavg [3]	0.05	-	-	5	-	-	-	94.31
HierFAVG [25]	0.05	-	-	5	4	-	-	95.05
HeurFedAMP [15]	0.05	0.05	-	5	-	0.1	97.65	-
	0.05	0.05	-	5	-	0.5	98.8	-
Fedprox [13]	0.05	-	0.001	5	-	-	-	90.04
PerFedavg [16]	0.05	-	-	5	-	-	78.15	-
	0.05	0.05	5	5	-	-	99.17	91.14
	0.05	0.05	15	5	-	-	99.38	91.60
pFedMe [14]	0.05	0.05	20	5	-	-	99.39	93.04
	0.05	0.05	25	5	-	-	98.72	89.47
	0.05	0.05	30	5	-	-	52.08	10.53
pFedGP [17]	0.05	-	-	5	-	-	99.18	-
	0.05	0.05	5	5	4	-	99.01	94.69
	0.05	0.05	15	5	4	-	98.04	94.06
Ours	0.05	0.05	20	5	4	-	99.08	97.66
	0.05	0.05	25	5	4	-	98.63	97.87
	0.05	0.05	30	5	4	-	98.32	97.94

Table 4: Results of all of algorithms on FMNIST with Setting 1.

Method	η_1	η_2	λ	K	E	α	Acc. (%)	
							PM	GM
Fedavg [3]	0.05	-	-	5	-	-	-	79.11
HierFAVG [25]	0.05	-	-	5	4	-	-	83.55
HeurFedAMP [15]	0.05	0.05	-	5	-	0.1	95.00	-
	0.05	0.05	-	5	-	0.5	98.28	-
Fedprox [13]	0.05	-	0.001	5	-	-	-	78.67
PerFedavg [16]	0.05	-	-	5	-	-	96.95	-
	0.05	0.05	5	5	-	-	98.84	79.76
	0.05	0.05	15	5	-	-	98.80	80.22
pFedMe [14]	0.05	0.05	20	5	-	-	98.81	79.66
	0.05	0.05	25	5	-	-	98.90	80.19
	0.05	0.05	30	5	-	-	98.94	80.57
pFedGP [17]	0.05	-	-	5	-	-	98.88	-
	0.05	0.05	5	5	4	-	98.55	84.01
	0.05	0.05	15	5	4	-	97.61	82.75
Ours	0.05	0.05	20	5	4	-	98.42	85.64
	0.05	0.05	25	5	4	-	95.86	86.51
	0.05	0.05	30	5	4	-	91.94	86.86

Table 5: Results of all of algorithms on FMNIST with Setting 2.

Method	η_1	η_2	λ	K	E	α	Acc. (%)	
							PM	GM
Fedavg [3]	0.05	-	-	5	-	-	-	84.48
HierFAVG [25]	0.05	-	-	5	4	-	-	85.48
HeurFedAMP [15]	0.05	0.05	-	5	-	0.1	97.43	-
	0.05	0.05	-	5	-	0.5	98.97	-
Fedprox [13]	0.05	-	0.001	5	-	-	-	84.33
PerFedavg [16]	0.05	-	-	5	-	-	96.47	-
	0.05	0.05	5	5	-	-	99.12	82.21
	0.05	0.05	15	5	-	-	99.14	82.18
pFedMe [14]	0.05	0.05	20	5	-	-	99.14	84.42
	0.05	0.05	25	5	-	-	99.17	85.14
	0.05	0.05	30	5	-	-	99.16	84.74
pFedGP [17]	0.05	-	-	5	-	-	99.20	-
	0.05	0.05	5	5	4	-	98.93	85.73
	0.05	0.05	15	5	4	-	98.5	83.7
Ours	0.05	0.05	20	5	4	-	98.98	89.29
	0.05	0.05	25	5	4	-	96.73	89.47
	0.05	0.05	30	5	4	-	93.35	89.05

Table 6: Results of all of algorithms on CIFAR with Setting 1.

Method	η_1	η_2	λ	K	E	α	Acc. (%)	
							PM	GM
Fedavg [3]	0.05	-	-	5	-	-	-	42.36
HierFAVG [25]	0.05	-	-	5	4	-	-	52.76
HeurFedAMP [15]	0.05	0.05	-	5	-	0.1	71.36	-
	0.05	0.05	-	5	-	0.5	82.26	-
Fedprox [13]	0.05	-	0.001	5	-	-	-	39.10
PerFedavg [16]	0.05	-	-	5	-	-	77.20	-
	0.05	0.05	5	5	-	-	85.46	34.75
	0.05	0.05	15	5	-	-	85.45	43.26
pFedMe [14]	0.05	0.05	20	5	-	-	87.33	48.25
	0.05	0.05	25	5	-	-	88.36	52.39
	0.05	0.05	30	5	-	-	88.45	58.66
pFedGP [17]	0.05	-	-	5	-	-	85.14	-
	0.05	0.05	5	5	4	-	78.00	47.91
	0.05	0.05	15	5	4	-	75.53	68.48
Ours	0.05	0.05	20	5	4	-	83.95	78.44
	0.05	0.05	25	5	4	-	76.98	65.83
	0.05	0.05	30	5	4	-	76.24	66.39

Table 7: Results of all of algorithms on CIFAR with Setting 2.

Method	η_1	η_2	λ	K	E	α	Acc. (%)	
							PM	GM
Fedavg [3]	0.05	-	-	5	-	-	-	81.74
HierFAVG [25]	0.05	-	-	5	4	-	-	87.28
HeurFedAMP [15]	0.05	0.05	-	5	-	0.1	83.51	-
	0.05	0.05	-	5	-	0.5	88.13	-
Fedprox [13]	0.05	-	0.001	5	-	-	-	72.98
PerFedavg [16]	0.05	-	-	5	-	-	84.92	-
pFedMe [14]	0.05	0.05	5	5	-	-	89.22	51.70
	0.05	0.05	15	5	-	-	90.08	62.06
	0.05	0.05	20	5	-	-	92.08	71.77
	0.05	0.05	25	5	-	-	93.17	86.95
	0.05	0.05	30	5	-	-	93.40	90.31
pFedGP [17]	0.05	-	-	5	-	-	85.98	-
Ours	0.05	0.05	5	5	4	-	88.44	83.17
	0.05	0.05	15	5	4	-	88.86	87.62
	0.05	0.05	20	5	4	-	92.39	92.42
	0.05	0.05	25	5	4	-	93.16	93.27
	0.05	0.05	30	5	4	-	93.98	94.09

Remark 4. For HeurFedAMP, we tune $\alpha \in [0.1, 0.5]$, where α represents the proportion of the client model that does not interact with the global model. For Fedprox, we tune $\lambda \in \{0.001, 0.01, 0.1, 1\}$ following the setting in [13]. For pFedMe and sFedHP, we use the same setting in [14] with $\lambda \in \{5, 15, 20, 25, 30\}$. For pFedGP, we use the same setting in [17] for other basic hyperparameters.

5 Conclusion

In this paper, we propose sFedHP as a sparse hierarchical personalized FL algorithm that can greatly remiss the statistical diversity issue to improve the FL performance and reduce the communication cost in FL. Our approach uses an approximated ℓ_1 -norm and the hierarchical proximal mapping to generate the loss function. The hierarchical proximal mapping enables the personalized edge-model, and client-model optimization can be decomposed from the global-model learning, which allows sFedHP parallelly optimizes the personalized edge-model and client-model by solving a tri-level problem. Theoretical results present that the sparse constraint in sFedHP only reduces the convergence speed to a small extent. In contrast, the simulation results show that the sparse constraint can significantly reduce the communication cost. Experimental results further demonstrate that sFedHP outperforms the client-edge-cloud hierarchical FedAvg and many other state-of-the-art personalized FL methods based on local customization under different settings.

Proof of the Results

.1 Proof of Lemma 1

Proof. First, we have

$$\begin{aligned}
\mathbb{E} \left[\|\mathbf{w}^{t+1} - \mathbf{w}^*\|^2 \right] &= \mathbb{E} \left[\|\mathbf{w}^t - \eta \mathbf{g}^t - \mathbf{w}^*\|_2^2 \right] \\
&= \mathbb{E} \left[\|\mathbf{w}^t - \mathbf{w}^*\|_2^2 \right] - 2\eta \mathbb{E} [\langle \mathbf{g}^t, \mathbf{w}^t - \mathbf{w}^* \rangle] + \eta^2 \mathbb{E} [\|\mathbf{g}^t\|_2^2]
\end{aligned} \tag{12}$$

and the second term of (12) is as follow

$$\begin{aligned}
& -\mathbb{E} \langle g^t, \mathbf{w}^T - \mathbf{w}^* \rangle \\
&= -\frac{1}{NR} \sum_{i,r}^{N,R} (\langle g_i^{t,r} - \nabla F_i(\mathbf{w}^t), \mathbf{w}^t - \mathbf{w}^* \rangle \\
&\quad + \langle \nabla F_i(\mathbf{w}^t), \mathbf{w}^t - \mathbf{w}^* \rangle) \\
&\stackrel{(a)}{\leq} \frac{1}{2NR} \sum_{i,r}^{N,R} \left(\frac{\|g_i^{t,r} - \nabla F_i(\mathbf{w}^t)\|_2^2}{\mu_F} + \mu_F \|\mathbf{w}^t - \mathbf{w}^*\|_2^2 \right) \\
&\quad - \frac{1}{NJ} \sum_{i,j=1}^{NJ} (\langle \nabla F_{i,j}(\mathbf{w}^t), \mathbf{w}^t - \mathbf{w}^* \rangle) \\
&\stackrel{(b)}{\leq} \frac{1}{2NR} \sum_{i,r}^{N,R} \left(\frac{\|g_i^{t,r} - \nabla F_i(\mathbf{w}^t)\|_2^2}{\mu_F} + \mu_F \|\mathbf{w}^t - \mathbf{w}^*\|_2^2 \right) \\
&\quad + \left(F(\mathbf{w}^*) - F(\mathbf{w}^t) - \frac{\mu_F}{2} \|\mathbf{w}^t - \mathbf{w}^*\|_2^2 \right) \\
&= \frac{1}{2NR} \sum_{i,r}^{N,R} \left(\frac{\|g_i^{t,r} - \nabla F_i(\mathbf{w}^t)\|_2^2}{\mu_F} \right) + F(\mathbf{w}^*) - F(\mathbf{w}^t). \tag{13}
\end{aligned}$$

where (a) follows by the Peter Paul inequality and the Jensen's inequality and (b) is due to Theorem 1.

From equations (18) and (19) in [14], we have

$$\begin{aligned}
\|g^t\|^2 &\leq \frac{3}{NR} \sum_{i,r}^{N,R} \|g_i^{t,r} - \nabla F_i(\mathbf{w}^t)\|_2^2 \\
&\quad + 3 \left\| \frac{1}{S} \sum_{i \in \mathcal{S}^t} \nabla F_i(\mathbf{w}^t) - \nabla F(\mathbf{w}^t) \right\|_2^2 \\
&\quad + 6L_F (F(\mathbf{w}^t) - F(\mathbf{w}^*)). \tag{14}
\end{aligned}$$

Taking expectation of the second term of (14) w.r.t edge server sampling, we have

$$\begin{aligned}
& \mathbb{E}_{S_t} \left\| \frac{1}{S} \sum_{i \in \mathcal{S}^t} \nabla F_i(\mathbf{w}^t) - \nabla F(\mathbf{w}^t) \right\|_2^2 \\
&\stackrel{(a)}{\leq} \frac{1}{SJ} \sum_{j=1}^J \mathbb{E}_{S_t} \left(\sum_{i \in \mathcal{S}^t} \|\nabla F_{i,j}(\mathbf{w}^t) - \nabla F(\mathbf{w}^t)\|_2^2 \right) \\
&\stackrel{(b)}{=} \frac{1}{SJ} \sum_{i,j}^{NJ} \left(\|\nabla F_{i,j}(\mathbf{w}^t) - \nabla F(\mathbf{w}^t)\|_2^2 \right) \mathbb{E}_{S_t} [\mathbb{I}_{i \in \mathcal{S}^t}] \\
&\leq \frac{1}{NJ} \sum_{i,j}^{NJ} \left(\|\nabla F_{i,j}(\mathbf{w}^t) - \nabla F(\mathbf{w}^t)\|_2^2 \right) \tag{15}
\end{aligned}$$

where (a) is due to the Jensen's inequality; \mathbb{I}_X in (b) is an indicator function of an event X ; and $\mathbb{E}_{S_t} [\mathbb{I}_{i \in \mathcal{S}^t}] = \frac{S}{N}$.

By substituting (13), (14), (15) into (12), we finish the proof of Lemma 1. \square

.2 Proof of Lemma 2

Proof. By noting that the last term of (10) only w.r.t. $\varphi_{i,j}^{t,r}$ we have

$$\begin{aligned}\check{\theta}_{i,j}(\varphi_{i,j}^{t,r}) &= \arg \min_{\theta_{i,j} \in \mathbb{R}^d} \check{\ell}_{i,j}(\theta_{i,j}) + \frac{\lambda_1}{2} \|\theta_{i,j} - \varphi_{i,j}^{t,r}\|_2^2 + \gamma_1 \phi_\rho(\theta_{i,j}). \\ \hat{\theta}_{i,j}(\varphi_{i,j}^{t,r}) &= \arg \min_{\theta_{i,j} \in \mathbb{R}^d} \hat{\ell}_{i,j}(\theta_{i,j}) + \frac{\lambda_1}{2} \|\theta_{i,j} - \varphi_{i,j}^{t,r}\|_2^2 + \gamma_1 \phi_\rho(\theta_{i,j}).\end{aligned}$$

Denote $h_{i,j}(\theta_{i,j}; \varphi_{i,j}^{t,r}) = \ell_{i,j}(\theta_{i,j}) + \gamma_1 \phi_\rho(\theta_{i,j}) + \frac{\lambda_1}{2} \|\theta_{i,j} - \varphi_{i,j}^{t,r}\|_2^2$. Then, $h_i(\theta_{i,j}; \varphi_{i,j}^{t,r})$ is $(\lambda_1 + \mu)$ -strongly convex when A.1(a) holds and $(\lambda_1 - L - \frac{\gamma_1}{\rho})$ -strongly convex when A.1(b) and $\lambda_1 > L + \frac{\gamma_1}{\rho}$ holds. Follow the proof in [14], we obtain the result in Lemma 2. \square

.3 Proof of Lemma 3

Proof.

$$\begin{aligned}& \mathbb{E} \left[\|g_i^{t,r} - \nabla F_i(\mathbf{w}^t)\|_2^2 \right] \\ & \stackrel{(a)}{\leq} 2\mathbb{E} \left[\|g_i^{t,r} - \nabla F_i(\mathbf{w}_i^{t,r})\|_2^2 + \|\nabla F_i(\mathbf{w}_i^{t,r}) - \nabla F_i(\mathbf{w}^t)\|_2^2 \right] \\ & \stackrel{(b)}{\leq} \frac{2}{J} \sum_{j=1}^J (\lambda_2^2 \mathbb{E} \left[\|\check{\varphi}_{i,j}^{t,r+1} - \hat{\varphi}_{i,j}^{t,r+1}\|_2^2 \right] + L_F^2 \mathbb{E} \left[\|\mathbf{w}_i^{t,r} - \mathbf{w}^t\|_2^2 \right]) \\ & \stackrel{(c)}{=} \frac{2}{J} \sum_{j=1}^J (\bar{\lambda}^2 \mathbb{E} \left[\|\check{\theta}_{i,j}^{t,r+1} - \hat{\theta}_{i,j}^{t,r+1}\|_2^2 \right] + L_F^2 \mathbb{E} \left[\|\mathbf{w}_i^{t,r} - \mathbf{w}^t\|_2^2 \right]) \\ & \leq 2 \left(\bar{\lambda}^2 \delta^2 + L_F^2 \mathbb{E} \left[\|\mathbf{w}_i^{t,r} - \mathbf{w}^t\|_2^2 \right] \right) \quad (16)\end{aligned}$$

where (a) follows by Jensen's inequality; (b) is due to Theorem 1, and (c) is due to the first-order conditions $\lambda_1(\hat{\varphi}_{i,j} - \check{\theta}_{i,j}) + \lambda_2(\hat{\varphi}_{i,j} - \mathbf{w}) = 0$ from (3) with $\bar{\lambda} = \frac{\lambda_1 \lambda_2}{\lambda_1 + \lambda_2}$. Moreover, the last term is bounded by

$$\begin{aligned}& \mathbb{E} \left[\|\mathbf{w}_i^{t,r} - \mathbf{w}^t\|_2^2 \right] \\ & \stackrel{(a)}{\leq} \frac{8\check{\eta}}{\beta L_F} \left(3\mathbb{E} \left[\|\nabla F_i(\mathbf{w}^t)\|_2^2 \right] + \frac{2\bar{\lambda}^2 \delta^2}{R} \right) \\ & \leq \frac{8\check{\eta}}{\beta L_F} \left(3\mathbb{E} \frac{1}{J} \sum_{j=1}^J \left[\|\nabla F_{i,j}(\mathbf{w}^t)\|_2^2 \right] + \frac{2\bar{\lambda}^2 \delta^2}{R} \right)\end{aligned}$$

where (a) follows by our proof of Lemma 2 in [31]. Thus we finish the proof of Lemma 3. \square

.4 Proof of Lemma 4

Proof. We first prove case (a), we have

$$\begin{aligned}& \frac{1}{NJ} \sum_{i=1,j=1}^{N,J} \|\nabla F_{i,j}(\mathbf{w}) - \nabla F(\mathbf{w})\|_2^2 \\ & \stackrel{(a)}{=} \frac{1}{NJ} \sum_{i,j=1}^{N,j} \|\nabla F_{i,j}(\mathbf{w})\|_2^2 - \left\| \frac{1}{NJ} \sum_{p,q=1}^N \nabla F_{i,j}(\mathbf{w}) \right\|_2^2 \\ & \stackrel{(b)}{\leq} \frac{2}{NJ} \sum_{i,j=1}^{N,J} \|\nabla F_{i,j}(\mathbf{w}) - \nabla F_{i,j}(\mathbf{w}^*)\|_2^2 + \|\nabla F_{i,j}(\mathbf{w}^*)\|_2^2 \\ & \stackrel{(c)}{\leq} 4L_F (F(\mathbf{w}) - F(\mathbf{w}^*)) + \frac{2}{NJ} \sum_{i,j=1}^N \|\nabla F_{i,j}(\mathbf{w}^*)\|_2^2\end{aligned}$$

where (a) follows by $\mathbb{E} [\|\mathbf{x} - \mathbb{E}[\mathbf{x}]\|_2^2] = \mathbb{E} [\|\mathbf{x}\|_2^2] - \mathbb{E} [\|\mathbf{x}\|_2]^2$; (b) follows by the Jensen's inequality; (c) follows by Theorem 1, thus F_i is μ_F -strong convex and L_F -smooth with $\nabla F(\mathbf{w}^*) = 0$.

We next prove case (b). For the minimization problem in (3), we have the first-order conditions $\lambda_1(\hat{\varphi}_{i,j} - \hat{\theta}_{i,j}) + \lambda_2(\hat{\varphi}_{i,j} - \mathbf{w}) = 0$ and $\nabla \ell_{i,j}(\hat{\theta}_{i,j}) - \lambda_1(\hat{\varphi}_{i,j} - \hat{\theta}_{i,j}) + \gamma_1 \nabla \phi_\rho(\hat{\theta}_{i,j}) = 0$, then we have

$$\begin{aligned} \nabla F_{i,j}(\mathbf{w}) &= \lambda_2(\mathbf{w} - \hat{\varphi}_{i,j}) + \gamma_2 \nabla \phi_\rho(\mathbf{w}) \\ &= \lambda_1(\hat{\varphi}_{i,j} - \hat{\theta}_{i,j}) + \gamma_2 \nabla \phi_\rho(\mathbf{w}) \\ &= \nabla \ell_{i,j}(\hat{\theta}_{i,j}) + \gamma_1 \nabla \phi_\rho(\hat{\theta}_{i,j}) + \gamma_2 \nabla \phi_\rho(\mathbf{w}) \\ &= \nabla L_{i,j}(\hat{\theta}_{i,j}) + \gamma_2 \nabla \phi_\rho(\mathbf{w}), \end{aligned} \tag{17}$$

where $L_{i,j}(\cdot) = \ell_{i,j}(\cdot) + \gamma_1 \phi_\rho(\cdot)$.

Hence, we have

$$\begin{aligned} & \|\nabla F_{i,j}(\mathbf{w}) - \nabla F(\mathbf{w})\|_2^2 \\ & \stackrel{(a)}{=} \left\| \nabla L_{i,j}(\hat{\theta}_{i,j}) - \frac{1}{NJ} \sum_{p,q=1}^{NJ} \nabla L_{p,q}(\hat{\theta}_{p,q}) \right\|_2^2 \\ & \stackrel{(b)}{\leq} 2 \left\| \nabla L_{i,j}(\hat{\theta}_{i,j}) - \frac{1}{NJ} \sum_{p,q=1}^{NJ} \nabla L_{p,q}(\hat{\theta}_{i,j}) \right\|_2^2 \\ & \quad + 2 \left\| \frac{1}{NJ} \sum_{p,q=1}^{NJ} \left(\nabla L_{p,q}(\hat{\theta}_{i,j}) - \nabla L_{p,q}(\hat{\theta}_{p,q}) \right) \right\|_2^2, \end{aligned}$$

where (a) follows by (17) and (b) follows by the Jensen's inequality. Taking the average over the number of clients, we have

$$\begin{aligned} & \frac{1}{NJ} \sum_{i,j=1}^{N,J} \|\nabla F_{i,j}(\mathbf{w}) - \nabla F(\mathbf{w})\|_2^2 \\ & \stackrel{(a)}{\leq} 2\sigma_\ell^2 + \frac{2}{N^2 J^2} \sum_{i,j=1}^{N,J} \sum_{p,q=1}^{N,J} \left\| \nabla L_{p,q}(\hat{\theta}_{i,j}) - \nabla L_{p,q}(\hat{\theta}_{p,q}) \right\|_2^2 \\ & \stackrel{(b)}{\leq} 2\sigma_\ell^2 + \frac{2(L + \frac{\gamma_1}{\rho})^2}{N^2 J^2} \sum_{i,j=1}^{N,J} \sum_{p,q=1}^{N,J} \left\| \hat{\theta}_{i,j} - \hat{\theta}_{p,q} \right\|_2^2, \end{aligned} \tag{18}$$

where (a) follows by Assumption 3 and the Jensen's inequality; (b) is due to the $(L + \frac{\gamma_1}{\rho})$ -smoothness of $L_{i,j}(\cdot)$; and the last term

$$\begin{aligned}
& \sum_{i,j=1}^{N,J} \sum_{p,q=1}^{N,J} \left\| \hat{\theta}_{i,j} - \hat{\theta}_{p,q} \right\|_2^2 \\
& \stackrel{(a)}{\leq} 4 \sum_{i,j=1}^{N,J} \sum_{p,q=1}^{N,J} \left(\left\| \hat{\theta}_{i,j} - \hat{\varphi}_{i,j} - \frac{\gamma_2}{\lambda_1} \nabla \phi_\rho(\mathbf{w}) \right\|_2^2 \right. \\
& \quad + \left\| \hat{\theta}_{p,q} - \hat{\varphi}_{p,q} - \frac{\gamma_2}{\lambda_1} \nabla \phi_\rho(\mathbf{w}) \right\|_2^2 \\
& \quad + \left\| \hat{\varphi}_{i,j} - \mathbf{w} - \frac{\gamma_2}{\lambda_2} \nabla \phi_\rho(\mathbf{w}) \right\|_2^2 \\
& \quad \left. + \left\| \hat{\varphi}_{p,q} - \mathbf{w} - \frac{\gamma_2}{\lambda_2} \nabla \phi_\rho(\mathbf{w}) \right\|_2^2 \right) \\
& \stackrel{(b)}{=} 4 \sum_{i,j=1}^{N,J} \sum_{p,q=1}^{N,J} \left(\frac{1}{\lambda_1^2} + \frac{1}{\lambda_2^2} \right) \left(\left\| \nabla F_{i,j}(\mathbf{w}) \right\|_2^2 + \left\| \nabla F_{p,q}(\mathbf{w}) \right\|_2^2 \right) \\
& \stackrel{(c)}{=} \frac{8NJ(\lambda_1^2 + \lambda_2^2)}{\lambda_1^2 \lambda_2^2} \sum_{i,j=1}^{N,J} \left\| \nabla F_{i,j}(\mathbf{w}) \right\|_2^2, \tag{19}
\end{aligned}$$

where (a) is due to the Jensen's inequality; (b) follows by (17); (c) follows by re-arranging the terms. Substituting (19) back to (18) we have

$$\begin{aligned}
& \frac{1}{NJ} \sum_{i,j=1}^{N,J} \left\| \nabla F_{i,j}(\mathbf{w}) - \nabla F(\mathbf{w}) \right\|_2^2 \\
& \leq 2\sigma_\ell^2 + \frac{16(L + \frac{\gamma_1}{\rho})^2(\lambda_1^2 + \lambda_2^2)}{NJ(\lambda_1^2 \lambda_2^2)} \sum_{i,j=1}^{N,J} \left\| \nabla F_{i,j}(\mathbf{w}) \right\|_2^2 \\
& \stackrel{(a)}{\leq} 2\sigma_\ell^2 + \frac{16(L + \frac{\gamma_1}{\rho})^2(\lambda_1^2 + \lambda_2^2)}{\lambda_1^2 \lambda_2^2} \left(\left\| \nabla F(\mathbf{w}) \right\|_2^2 \right. \\
& \quad \left. + \frac{1}{NJ} \sum_{i,j=1}^{N,J} \left\| \nabla F_{i,j}(\mathbf{w}) - \nabla F(\mathbf{w}) \right\|_2^2 \right) \\
& \stackrel{(b)}{\leq} \frac{16(L + \frac{\gamma_1}{\rho})^2}{\lambda^2 - 16(L + \frac{\gamma_1}{\rho})^2} \left\| \nabla F(\mathbf{w}) \right\|_2^2 + \frac{2\lambda^2}{\lambda^2 - 16(L + \frac{\gamma_1}{\rho})^2} \sigma_\ell^2,
\end{aligned}$$

where (a) follows by the equation $\mathbb{E} [\| \mathbf{x} - \mathbb{E} [\mathbf{x}] \|_2^2] = \mathbb{E} [\| \mathbf{x} \|_2^2] - \mathbb{E} [\| \mathbf{x} \|_2]^2$; (b) is by re-arranging the terms with setting $\lambda = \frac{\lambda_1 \lambda_2}{\sqrt{\lambda_1^2 + \lambda_2^2}}$. \square

5 Proof of Theorem 1

Proof. We first prove some interesting character of $\phi_\rho(\mathbf{x})$ in (4), which is convex smooth approximation to $\| \mathbf{x} \|_1$ [26] and

$$0 \leq \nabla^2 \phi_\rho(x) = \frac{1}{\rho} \left(1 - (\tanh(x/\rho))^2 \right) \leq \frac{1}{\rho},$$

which yields $\nabla\phi_\rho(x) - \nabla\phi_\rho(\bar{x}) \leq \frac{1}{\rho}(x - \bar{x})$, then we have

$$\begin{aligned} & \|\nabla\phi_\rho(\mathbf{x}) - \nabla\phi_\rho(\bar{\mathbf{x}})\|_2 \\ &= \sqrt{\sum_{n=1}^d (\tanh(x_n/\rho) - \tanh(\bar{x}_n/\rho))^2} \\ &\leq \frac{1}{\rho} \sqrt{\sum_{n=1}^d (x_n - \bar{x}_n)^2} = \frac{1}{\rho} \|\mathbf{x} - \bar{\mathbf{x}}\|_2. \end{aligned}$$

Hence, ϕ_ρ is convex function with $\frac{1}{\rho}$ -Lipschitz $\nabla\phi_\rho$.

Let $L_{i,j}(\boldsymbol{\theta}_{i,j}) = \ell_{i,j}(\boldsymbol{\theta}_{i,j}) + \gamma_1\phi_\rho(\boldsymbol{\theta}_{i,j})$. On the one hand if $\ell_{i,j}$ is μ -strong convex. For $\alpha \in [0, 1]$, we hence have

$$\begin{aligned} & \ell_{i,j}(\alpha\boldsymbol{\theta}_{i,j} + (1-\alpha)\bar{\boldsymbol{\theta}}_{i,j}) \\ &\leq \alpha\ell_{i,j}(\boldsymbol{\theta}_{i,j}) + (1-\alpha)\ell_{i,j}(\bar{\boldsymbol{\theta}}_{i,j}) - \frac{\mu}{2}\alpha(1-\alpha)\|\boldsymbol{\theta}_{i,j} - \bar{\boldsymbol{\theta}}_{i,j}\|_2. \end{aligned} \tag{20}$$

In addition, by noting that ϕ_ρ is convex function, we have

$$\phi_\rho(\alpha\boldsymbol{\theta}_{i,j} + (1-\alpha)\bar{\boldsymbol{\theta}}_{i,j}) \leq \alpha\phi_\rho(\boldsymbol{\theta}_{i,j}) + (1-\alpha)\phi_\rho(\bar{\boldsymbol{\theta}}_{i,j}). \tag{21}$$

Combining (20) and (21) yields

$$\begin{aligned} & \ell_{i,j}(\alpha\boldsymbol{\theta}_{i,j} + (1-\alpha)\bar{\boldsymbol{\theta}}_{i,j}) \\ &\leq \alpha L_{i,j}(\boldsymbol{\theta}_{i,j}) + (1-\alpha)L_{i,j}(\bar{\boldsymbol{\theta}}_{i,j}) - \frac{\mu}{2}\alpha(1-\alpha)\|\boldsymbol{\theta}_{i,j} - \bar{\boldsymbol{\theta}}_{i,j}\|_2, \end{aligned}$$

which shows that if $\ell_{i,j}$ is μ -strong convex, $L_{i,j}(\boldsymbol{\theta}_{i,j}) = \ell_{i,j}(\boldsymbol{\theta}_{i,j}) + \gamma_1\phi_\rho(\boldsymbol{\theta}_{i,j})$ is μ -strong convex.

On the other hand, if $\ell_{i,j}$ is nonconvex with L -Lipschitz $\nabla\ell_{i,j}$, we have

$$\begin{aligned} & \|\nabla L_{i,j}(\boldsymbol{\theta}_{i,j}) - \nabla L_{i,j}(\bar{\boldsymbol{\theta}}_{i,j})\|_2 \\ &= \|\nabla\ell_{i,j}(\boldsymbol{\theta}_{i,j}) - \nabla\ell_{i,j}(\bar{\boldsymbol{\theta}}_{i,j}) + \gamma_1\nabla\phi_\rho(\boldsymbol{\theta}_{i,j}) - \gamma_1\nabla\phi_\rho(\bar{\boldsymbol{\theta}}_{i,j})\|_2 \\ &\leq \|\nabla\ell_{i,j}(\boldsymbol{\theta}_{i,j}) - \nabla\ell_{i,j}(\bar{\boldsymbol{\theta}}_{i,j})\|_2 + \gamma_1\|\nabla\phi_\rho(\boldsymbol{\theta}_{i,j}) - \nabla\phi_\rho(\bar{\boldsymbol{\theta}}_{i,j})\|_2 \\ &\leq (L + \frac{\gamma_1}{\rho})\|\mathbf{w} - \bar{\mathbf{w}}\|_2, \end{aligned}$$

which shows that if $\ell_{i,j}$ is L -smooth, then $L_{i,j}(\boldsymbol{\theta}_{i,j}) = \ell_{i,j}(\boldsymbol{\theta}_{i,j}) + \gamma_1\phi_\rho(\boldsymbol{\theta}_{i,j})$ is $L + \frac{\gamma_1}{\rho}$ -smooth.

Let $g(\boldsymbol{\varphi}_{i,j}) = M_{L_{i,j}}^{\boldsymbol{\theta}_{i,j}}(\boldsymbol{\varphi}_{i,j}) = \min_{\boldsymbol{\theta}_{i,j} \in \mathbb{R}^d} L_{i,j}(\boldsymbol{\theta}_{i,j}) + \frac{\lambda_1}{2}\|\boldsymbol{\varphi}_{i,j} - \boldsymbol{\theta}_{i,j}\|_2^2$, which is the famous Moreau envelope [27], thus if $L_{i,j}$ is convex or nonconvex but $(L + \frac{\gamma_1}{\rho})$ -smooth, then $g(\boldsymbol{\varphi}_{i,j})$ is L_g -smooth with $L_g = \lambda_1$ (with the condition that $\lambda_1 > 2(L + \frac{\gamma_1}{\rho})$ for nonconvex $L + \frac{\gamma_1}{\rho}$ -smooth). Therefore if $L_{i,j}$ is μ -strong convex, $g(\boldsymbol{\varphi}_{i,j})$ is μ_g -strong convex with $\mu_g = \frac{\lambda_1\mu}{\lambda_1 + \mu}$.

Let $G_{i,j}(\mathbf{w}) = M_{g_{i,j}}^{\boldsymbol{\varphi}_{i,j}}(\boldsymbol{\varphi}_{i,j}) = \min_{\boldsymbol{\varphi}_{i,j} \in \mathbb{R}^d} g_{i,j}(\boldsymbol{\varphi}_{i,j}) + \frac{\lambda_2}{2}\|\mathbf{w} - \boldsymbol{\varphi}_{i,j}\|_2^2$, similarly we have if $g_{i,j}$ is convex or nonconvex with L_g -smooth, then $G_{i,j}(\mathbf{w})$ is L_G -smooth with $L_G = \lambda_2$ (with the condition that $\lambda_2 > 2L_g$ for nonconvex L_g -smooth). Therefore if $g_{i,j}$ is μ_g -strong convex, yeilds $G_{i,j}(\mathbf{w})$ is μ_G -strong convex with

$$\mu_G = \frac{\lambda_2\mu_g}{\lambda_2 + \mu_g} = \frac{\lambda_1\lambda_2\mu}{\lambda_1\mu + \lambda_2\mu + \lambda_1\lambda_2}.$$

Furthermore, recall that

$$\begin{aligned} F_{i,j}(\mathbf{w}) &= \min_{\boldsymbol{\varphi}_{i,j}, \boldsymbol{\theta}_{i,j} \in \mathbb{R}^d} \ell_{i,j}(\boldsymbol{\theta}_{i,j}) + \frac{\lambda_1}{2}\|\boldsymbol{\theta}_{i,j} - \boldsymbol{\varphi}_{i,j}\|_2^2 \\ &\quad + \gamma_1\phi_\rho(\boldsymbol{\theta}_{i,j}) + \frac{\lambda_2}{2}\|\boldsymbol{\varphi}_{i,j} - \mathbf{w}\|_2^2 + \gamma_2\phi_\rho(\mathbf{w}) \\ &= \min_{\boldsymbol{\varphi}_{i,j} \in \mathbb{R}^d} g_{i,j}(\boldsymbol{\varphi}_{i,j}) + \frac{\lambda_2}{2}\|\mathbf{w} - \boldsymbol{\varphi}_{i,j}\|_2^2 + \gamma_2\phi_\rho(\mathbf{w}) \\ &= G(\mathbf{w}) + \gamma_2\phi_\rho(\mathbf{w}). \end{aligned}$$

Using the character of ϕ_ρ mentioned before, we have the similarly conclusion that if G_i is μ_G -strongly convex, $F_{i,j}$ is μ_F -strong convex with $\mu_F = \mu_G = \frac{\lambda_1 \lambda_2 \mu}{\lambda_1 \mu + \lambda_2 \mu + \lambda_1 \lambda_2}$, and if G_i is L_G -smooth, $F_{i,j}$ is L_F -smooth with $L_F = L_G + \frac{\gamma_2}{\rho} = \lambda_2 + \frac{\gamma_2}{\rho}$. Finally, combining the first-order condition $\lambda_1(\hat{\varphi}_{i,j} - \hat{\theta}_{i,j}) + \lambda_2(\hat{\varphi}_{i,j} - \mathbf{w}) = 0$, we complete the proof. \square

.6 Proof of Theorem 2

Proof. Let $\check{\eta} \leq \min \left\{ \frac{1}{\mu_F}, \frac{1}{3L_F(3+128L_F/(\mu_F\beta))} \right\}$ hold, combining Lemma 3 and Lemma 4 with Lemma 1 yields

$$\begin{aligned} & \mathbb{E} [\|\mathbf{w}^{t+1} - \mathbf{w}^*\|_2^2] \\ & \leq \Delta_t - \check{\eta} M \mathbb{E} [F(\mathbf{w}^t) - F(\mathbf{w}^*)] + \check{\eta} M_1 + \check{\eta}^2 M_2 \\ & \stackrel{(a)}{\leq} \Delta_t - \check{\eta} \mathbb{E} [F(\mathbf{w}^t) - F(\mathbf{w}^*)] + \check{\eta} M_1 + \check{\eta}^2 M_2, \end{aligned}$$

where Δ_t denotes $\mathbb{E} [\|\mathbf{w}^t - \mathbf{w}^*\|_2^2]$, $M = 2 - \check{\eta} L_F(18 + \frac{768L_F}{\mu_F\beta})$, $M_1 = \frac{8\delta^2\lambda^2}{\mu_F}$, $M_2 = 6(1 + 64\frac{L_F}{\mu_F\beta})\sigma_{F,1}^2 + \frac{128L_F\delta^2\lambda^2}{\mu_F\beta}$, and (a) is due to $\check{\eta} \leq \frac{1}{3L_F(3+128L_F/(\mu_F\beta))}$, then

$$\begin{aligned} \frac{1}{T} \sum_{t=0}^{T-1} \mathbb{E} [F(\mathbf{w}^t) - F(\mathbf{w}^*)] & \leq \frac{1}{\check{\eta}T} (\Delta_0 - \Delta_T) + M_1 + \check{\eta} M_2 \\ & \leq \frac{\Delta_0}{\check{\eta}T} + M_1 + \check{\eta} M_2. \end{aligned} \tag{22}$$

Then, the proof of part (a) is finished.

We next prove the part (b), we have

$$\begin{aligned} & \mathbb{E} [\|\check{\theta}_{i,j}^T - \mathbf{w}^*\|_2^2] \\ & \stackrel{(a)}{\leq} 5 \mathbb{E} \left(\left\| \check{\theta}_{i,j}^T - \hat{\theta}_{i,j}^T \right\|_2^2 + \left\| \hat{\theta}_{i,j}^T - \hat{\varphi}_{i,j}^T - \frac{\gamma_2}{\lambda_1} \nabla \phi_\rho(\mathbf{w}^T) \right\|_2^2 \right. \\ & \quad + \left\| \hat{\varphi}_{i,j}^T - \mathbf{w}^T - \frac{\gamma_2}{\lambda_2} \nabla \phi_\rho(\mathbf{w}^T) \right\|_2^2 + \|\mathbf{w}^T - \mathbf{w}^*\|_2^2 \\ & \quad \left. + \left\| \frac{\gamma_2(\lambda_1 + \lambda_2)}{\lambda_1 \lambda_2} \nabla \phi_\rho(\mathbf{w}^T) \right\|_2^2 \right) \\ & \stackrel{(b)}{\leq} 5 \left(\delta^2 + \frac{1}{\lambda^2} \mathbb{E} [\|\nabla F_{i,j}(\mathbf{w}^T)\|_2^2] + \mathbb{E} [\|\mathbf{w}^T - \mathbf{w}^*\|_2^2] \right. \\ & \quad \left. + \frac{\gamma_2^2}{\lambda^2} \mathbb{E} [\|\nabla \phi_\rho(\mathbf{w}^T)\|_2^2] \right) \\ & \stackrel{(c)}{\leq} 5 \left(\delta^2 + \frac{\gamma_2^2}{\lambda^2} \mathbb{E} [\|\nabla \phi_\rho(\mathbf{w}^T)\|_2^2] + \mathbb{E} [\|\mathbf{w}^T - \mathbf{w}^*\|_2^2] \right) \\ & \quad + \frac{10}{\lambda^2} \mathbb{E} \left[\|\nabla F_{i,j}(\mathbf{w}^T) - \nabla F_{i,j}(\mathbf{w}^*)\|_2^2 \right. \\ & \quad \left. + \|\nabla F_{i,j}(\mathbf{w}^*)\|_2^2 \right] \\ & \stackrel{(d)}{\leq} 5 \left(\delta^2 + \frac{\gamma_2^2}{\lambda^2} \mathbb{E} [\|\nabla \phi_\rho(\mathbf{w}^T)\|_2^2] + \mathbb{E} [\|\mathbf{w}^T - \mathbf{w}^*\|_2^2] \right) \\ & \quad + \frac{10}{\lambda^2} \mathbb{E} \left[L_F \|\mathbf{w}^T - \mathbf{w}^*\|_2^2 + \|\nabla F_{i,j}(\mathbf{w}^*)\|_2^2 \right], \end{aligned} \tag{23}$$

where (a) and (c) are due to the Jensen's inequality; (b) is due to (17); and (d) is due to Theorem 1. In addition, the second term of (23) is bounded by

$$\mathbb{E} \left[\left\| \nabla \phi_\rho(\mathbf{w}^T) \right\|_2^2 \right] = \mathbb{E} \left[\sum_{i=1}^d \left(\frac{\sinh(|w_n^T|/\rho)}{\cosh(|w_n^T|/\rho)} \frac{w_n^T}{|w_n^T|} \right)^2 \right] \quad (24)$$

$$\leq \mathbb{E} \left[\sum_{i=1}^d \left(\frac{w_n^T}{|w_n^T|} \right)^2 \right] \\ = d_s^2, \quad (25)$$

where $\frac{\sinh(|w_n^T|/\rho)}{\cosh(|w_n^T|/\rho)} \in (-1, 1)$, w_n^T is the n -th element of \mathbf{w}^T and d_s denotes the number of non-zero elements in \mathbf{w} . Due to the μ_F -strong convex of F , we have

$$\mathbb{E} \left[\left\| \mathbf{w}^T - \mathbf{w}^* \right\|_2^2 \right] \leq \frac{2(\mathbb{E}[F(\mathbf{w}_T)] - F(\mathbf{w}^*))}{\mu_F}. \quad (26)$$

By substituting (22), (25) and (26) into (23) we complete the proof. \square

7 Proof of Theorem 3

Proof. We first prove part (a). Similar with the proof in [14], we rewrite the recursive formula due to the L -smooth of $F(\cdot)$

$$\begin{aligned} & \mathbb{E} [F(\mathbf{w}^{t+1}) - F(\mathbf{w}^t)] \\ & \leq \mathbb{E} [\langle \nabla F(\mathbf{w}^t), \mathbf{w}^{t+1} - \mathbf{w}^t \rangle] + \frac{L_F}{2} \mathbb{E} [\left\| \mathbf{w}^{t+1} - \mathbf{w}^t \right\|_2^2] \\ & = -\check{\eta} \mathbb{E} [\langle \nabla F(\mathbf{w}^t), g^t \rangle] + \frac{\check{\eta}^2 L_F}{2} \mathbb{E} [\left\| g^t \right\|_2^2] \\ & = -\check{\eta} \mathbb{E} [\left\| \nabla F(\mathbf{w}^t) \right\|_2^2] - \check{\eta} \mathbb{E} [\langle \nabla F(\mathbf{w}^t), g^t - \nabla F(\mathbf{w}^t) \rangle] \\ & \quad + \frac{\check{\eta}^2 L_F}{2} \mathbb{E} [\left\| g^t \right\|_2^2] \\ & \stackrel{(b)}{\leq} -\check{\eta} \mathbb{E} [\left\| \nabla F(\mathbf{w}^t) \right\|_2^2] + \frac{\check{\eta}}{2} \mathbb{E} [\left\| \nabla F(\mathbf{w}^t) \right\|_2^2] \\ & \quad + \frac{\check{\eta}}{2} \mathbb{E} \left\| \frac{1}{NR} \sum_{i,r}^{N,R} g_{i,r}^t - \nabla F_i(\mathbf{w}^t) \right\|_2^2 + \frac{\check{\eta}^2 L_F}{2} \mathbb{E} [\left\| g^t \right\|_2^2] \\ & \stackrel{(c)}{\leq} -\frac{\check{\eta}(1 - 3L_F\check{\eta})}{2} \mathbb{E} [\left\| \nabla F(\mathbf{w}_t) \right\|_2^2] \\ & \quad + \frac{\check{\eta}(1 + 3L_F\check{\eta})}{2} \mathbb{E} \left\| \frac{1}{NR} \sum_{i,r}^{N,R} g_{i,r}^t - \nabla F_i(\mathbf{w}^t) \right\|_2^2 \\ & \quad + \frac{3\check{\eta}^2 L_F}{2} \mathbb{E} \left\| \frac{1}{S} \sum_{i \in \mathcal{S}^t} \nabla F_i(\mathbf{w}^t) - \nabla F(\mathbf{w}^t) \right\|_2^2 \\ & \stackrel{(d)}{\leq} -\check{\eta} G \mathbb{E} [\left\| \nabla F(\mathbf{w}^t) \right\|_2^2] + \check{\eta} G_1 + \check{\eta}^2 G_2. \end{aligned}$$

where (b) is due to the Cauchy-Swartz inequalities; (c) is due to the Jensen's inequality; (d) follows by $1 + 3L_F\check{\eta} \leq 3\beta$ since $\check{\eta} \leq \frac{\beta}{2L_F}$, and $G_1 = 3\beta\bar{\lambda}^2\delta^2$, $G_2 = \frac{3L_F(49R\sigma_{F,2}^2 + 16\delta^2\bar{\lambda}^2)}{R}$.

Next, let $\lambda^2 - 16(L + \frac{\gamma_1}{\rho})^2 \geq 1$ and $\check{\eta} \leq \frac{1}{588L_F\lambda^2}$ hold, we have

$$\begin{aligned} G &= \frac{1}{2} - \check{\eta}L_F \left(\frac{3}{2} + \frac{24(L + \frac{\gamma_1}{\rho})^2}{\lambda^2 - 16(L + \frac{\gamma_1}{\rho})^2} + \frac{72\lambda^2}{\lambda^2 - 16(L + \frac{\gamma_1}{\rho})^2} \right) \\ &\geq \frac{1}{2} - \frac{147\check{\eta}L_F\lambda^2}{2} \geq \frac{1}{4}, \end{aligned}$$

we hence have

$$\begin{aligned} &\frac{1}{T} \sum_{t=0}^{T-1} \mathbb{E} \left[\|\nabla F(\mathbf{w}^t)\|^2 \right] \\ &\leq 4 \left(\frac{\mathbb{E} [F(\mathbf{w}^0) - F(\mathbf{w}^T)]}{\check{\eta}T} + G_1 + \check{\eta}^1 G_2 \right). \\ &\leq 4 \left(\frac{\Delta_F}{\check{\eta}T} + G_1 + \check{\eta}^1 G_2 \right), \end{aligned}$$

where $\Delta_F \triangleq F(\mathbf{w}^0) - F(W^*)$.

We next prove part (b), we have

$$\begin{aligned} &\frac{1}{NJ} \sum_{i,j=1}^{NJ} \mathbb{E} \left[\|\check{\theta}_{i,j}^t(\mathbf{w}^t) - \mathbf{w}^t\|_2^2 \right] \\ &\stackrel{(a)}{\leq} \frac{4}{NJ} \sum_{i,j=1}^{NJ} \mathbb{E} \left(\left\| \check{\theta}_{i,j}^t - \hat{\theta}_{i,j}^t \right\|_2^2 + \left\| \hat{\theta}_{i,j}^t - \hat{\varphi}_{i,j}^t - \frac{\gamma_2}{\lambda_1} \nabla \phi_\rho(\mathbf{w}^t) \right\|_2^2 \right. \\ &\quad \left. + \left\| \hat{\varphi}_{i,j}^t - \mathbf{w}^t - \frac{\gamma_2}{\lambda_2} \nabla \phi_\rho(\mathbf{w}^t) \right\|_2^2 + \left\| \frac{\gamma_2(\lambda_1 + \lambda_2)}{\lambda_1 \lambda_2} \nabla \phi_\rho(\mathbf{w}^t) \right\|_2^2 \right) \\ &\stackrel{(b)}{\leq} 4 \left(\delta^2 + \frac{\lambda_1^2 + \lambda_2^2}{\lambda_1^2 \lambda_2^2} \frac{1}{NJ} \sum_{i,j=1}^{NJ} \mathbb{E} \left[\|\nabla F_{i,j}(\mathbf{w}^t)\|_2^2 \right] \right. \\ &\quad \left. + \frac{\gamma_2^2(\lambda_1 + \lambda_2)^2}{\lambda_1^2 \lambda_2^2} \frac{1}{NJ} \sum_{i,j=1}^{NJ} \mathbb{E} \left[\|\nabla \phi_\rho(\mathbf{w}^t)\|_2^2 \right] \right) \\ &= 4 \left(\delta^2 + \frac{1}{\lambda^2} \frac{1}{NJ} \sum_{i,j=1}^{NJ} \mathbb{E} \left[\|\nabla F_{i,j}(\mathbf{w}^t)\|_2^2 \right] + \frac{\gamma_2^2}{\lambda^2} d_s^2 \right) \end{aligned} \tag{27}$$

where (a) is due to the Jensen's inequality, (b) is due to (17). And the last term is bounded by

$$\begin{aligned} &\frac{1}{NJ} \sum_{i,j=1}^{NJ} \mathbb{E} \left[\|\nabla F_{i,j}(\mathbf{w}^t)\|_2^2 \right] \\ &\stackrel{(a)}{=} \frac{1}{NJ} \sum_{i,j=1}^{NJ} \mathbb{E} \left[\|\nabla F_{i,j}(\mathbf{w}^t) - \nabla F(\mathbf{w}^t)\|_2^2 + \|\nabla F(\mathbf{w}^t)\|_2^2 \right] \\ &\stackrel{(b)}{\leq} \sigma_{F,2}^2 + \frac{\lambda^2}{\lambda^2 - 16(L + \frac{\gamma_1}{\rho})^2} \mathbb{E} \left[\|\nabla F(\mathbf{w}^t)\|_2^2 \right] \\ &\stackrel{(c)}{\leq} \sigma_{F,2}^2 + \lambda^2 \mathbb{E} \left[\|\nabla F(\mathbf{w}^t)\|_2^2 \right] \end{aligned} \tag{28}$$

where (a) is due to the equation $\mathbb{E} [\|\mathbf{x} - \mathbb{E}[\mathbf{x}]\|_2^2] = \mathbb{E} [\|\mathbf{x}\|_2^2] - \mathbb{E} [\|\mathbf{x}\|_2]^2$, (b) follows by Lemma 4, (c) is by setting $\lambda^2 - 16(L + \frac{\gamma_1}{\rho})^2 \leq 1$. By substituting (28) into (27), we finished the proof. \square

References

- [1] Yann LeCun, Yoshua Bengio, and Geoffrey Hinton. Deep learning. *nature*, 521(7553):436–444, 2015.
- [2] Jiasi Chen and Xukan Ran. Deep learning with edge computing: A review. *Proc. of the IEEE*, 107(8):1655–1674, 2019.
- [3] Brendan McMahan, Eider Moore, Daniel Ramage, Seth Hampson, and Blaise Aguera y Arcas. Communication-efficient learning of deep networks from decentralized data. In *Proc. of Artificial Intelligence and Statistics*, pages 1273–1282, 2017.
- [4] Yuanming Shi, Kai Yang, Tao Jiang, Jun Zhang, and Khaled B. Letaief. Communication-efficient edge ai: Algorithms and systems. *IEEE Communications Surveys Tutorials*, 22(4):2167–2191, 2020.
- [5] Mingzhe Chen, Zhaoxiang Yang, Walid Saad, Changchuan Yin, H. Vincent Poor, and Shuguang Cui. A joint learning and communications framework for federated learning over wireless networks. *IEEE Transactions on Wireless Communications*, 20(1):269–283, 2021.
- [6] Junqing Le, Xinyu Lei, Nankun Mu, Hengrun Zhang, Kai Zeng, and Xiaofeng Liao. Federated continuous learning with broad network architecture. *IEEE Transactions on Cybernetics*, 51(8):3874–3888, 2021.
- [7] Shiva Raj Pokhrel and Jinho Choi. Federated learning with blockchain for autonomous vehicles: Analysis and design challenges. *IEEE Transactions on Communications*, 68(8):4734–4746, 2020.
- [8] Le Zhang, Wei Cui, Bing Li, Zhenghua Chen, Min Wu, and Teo Sin Gee. Privacy-preserving cross-environment human activity recognition. *IEEE Transactions on Cybernetics*, pages 1–11, 2021.
- [9] Daliang Li and Junpu Wang. Fedmd: Heterogenous federated learning via model distillation. *arXiv preprint arXiv:1910.03581*, 2019.
- [10] Yuyang Deng, Mohammad Mahdi Kamani, and Mehrdad Mahdavi. Adaptive personalized federated learning. *arXiv preprint arXiv:2003.13461*, 2020.
- [11] Felix Sattler, Klaus-Robert Müller, and Wojciech Samek. Clustered federated learning: Model-agnostic distributed multitask optimization under privacy constraints. *IEEE Transactions on Neural Networks and Learning Systems*, 32(8):3710–3722, 2021.
- [12] Manoj Ghuhan Arivazhagan, Vinay Aggarwal, Aaditya Kumar Singh, and Sunav Choudhary. Federated learning with personalization layers. *arXiv preprint arXiv:1912.00818*, 2019.
- [13] Tian Li, Anit Kumar Sahu, Manzil Zaheer, Maziar Sanjabi, Ameet Talwalkar, and Virginia Smith. Federated optimization in heterogeneous networks. *arXiv preprint arXiv:1812.06127*, 2018.
- [14] Canh T. Dinh, Nguyen Tran, and Josh Nguyen. Personalized federated learning with moreau envelopes. In *Advances in Neural Information Processing Systems*, volume 33, pages 21394–21405, 2020.
- [15] Yutao Huang, Lingyang Chu, Zirui Zhou, Lanjun Wang, Jiangchuan Liu, Jian Pei, and Yong Zhang. Personalized cross-silo federated learning on non-iid data. In *Proc. of Association for the Advancement of Artificial Intelligence*, volume 35, pages 7865–7873, 2021.
- [16] Alireza Fallah, Aryan Mokhtari, and Asuman Ozdaglar. Personalized federated learning: A meta-learning approach. *arXiv preprint arXiv:2002.07948*, 2020.
- [17] Idan Achituv, Aviv Shamsian, Aviv Navon, Gal Chechik, and Ethan Fetaya. Personalized federated learning with gaussian processes. In *Advances in Neural Information Processing Systems*, volume 34, pages 8392–8406, 2021.
- [18] Suraj Srinivas, Akshayvarun Subramanya, and R Venkatesh Babu. Training sparse neural networks. In *Proc. of the IEEE Conference on Computer Vision and Pattern Recognition Workshops*, pages 138–145, 2017.
- [19] Song Han, Jeff Pool, John Tran, and William Dally. Learning both weights and connections for efficient neural network. *Advances in Neural Information Processing Systems*, 28:1135–1143, 2015.
- [20] Trevor Gale, Erich Elsen, and Sara Hooker. The state of sparsity in deep neural networks. *arXiv preprint arXiv:1902.09574*, 2019.
- [21] Nir Shlezinger, Mingzhe Chen, Yonina C. Eldar, H. Vincent Poor, and Shuguang Cui. Uveqfed: Universal vector quantization for federated learning. *IEEE Transactions on Signal Processing*, 69:500–514, 2021.
- [22] Felix Sattler, Simon Wiedemann, Klaus-Robert Müller, and Wojciech Samek. Robust and communication-efficient federated learning from non-i.i.d. data. *IEEE Transactions on Neural Networks and Learning Systems*, 31(9):3400–3413, 2020.
- [23] Kai Yue, Richeng Jin, Chau-Wai Wong, and Huaiyu Dai. Communication-efficient federated learning via predictive coding. *IEEE Journal of Selected Topics in Signal Processing*, 16(3):369–380, 2022.

- [24] Sai Praneeth Karimireddy, Satyen Kale, Mehryar Mohri, Sashank Reddi, Sebastian Stich, and Ananda Theertha Suresh. Scaffold: Stochastic controlled averaging for federated learning. In *Proc. of International Conference on Machine Learning*, pages 5132–5143, 2020.
- [25] Lumin Liu, Jun Zhang, SH Song, and Khaled B Letaief. Client-edge-cloud hierarchical federated learning. In *Proc. of IEEE International Conference on Communications*, pages 1–6. IEEE, 2020.
- [26] J. Sun, Q. Qu, and J. Wright. Complete dictionary recovery over the sphere i: Overview and the geometric picture. *IEEE Transactions on Information Theory*, 63(2):853–884, 2017.
- [27] Amir Beck. *First-order methods in optimization*. SIAM, 2017.
- [28] Yann LeCun, Léon Bottou, Yoshua Bengio, and Patrick Haffner. Gradient-based learning applied to document recognition. *Proc. of the IEEE*, 86(11):2278–2324, 1998.
- [29] Han Xiao, Kashif Rasul, and Roland Vollgraf. Fashion-mnist: a novel image dataset for benchmarking machine learning algorithms. *arXiv preprint arXiv:1708.07747*, 2017.
- [30] A Krizhevsky. Learning multiple layers of features from tiny images. *Master’s thesis, University of Tront*, 2009.
- [31] Xiaofeng Liu, Yinchuan Li, Xu Zhang, Yunfeng Shao, Qing Wang, and Yanhui Geng. Personalized federated learning via maximizing correlation. *arXiv preprint arXiv:2107.05330v3*, 2021.